ADAPTIVE KNOT LOCATION FOR SPLINE APPROXIMATION

by

Alberto Mauricio Mier Muth

S.B., Universidad Nacional Autonoma de Mexico

1974

SUBMITTED IN PARTIAL FULFILLMENT OF THE

REQUIREMENTS FOR THE DEGREE OF

MASTER OF SCIENCE

at the

MASSACHUSETTS INSTITUTE OF TECHNOLOGY

August, 1976

Signature of Author . . . . . .

Department of Electrical Engineering and
Computer Science, August 9, 1976.

Certified by . . . . . .

Thesis Supervisor

Accepted by . . . . . .

Chairman, Departmental Committee on Graduate Students

ADAPTIVE KNOT LOCATION FOR SPLINE APPROXIMATION

by

Alberto Mauricio Mier Muth

Submitted to the Department of Electrical Engineering and Computer Science on 9 August 1976 in partial fulfillment of the requirements for the Degree of Master of Science

ABSTRACT

The Constrained generalized likelihood ratio (CGLR) technique is applied to the problem of locating knots in a spline approximation. Theoretical - analysis is performed to determine performance tradeoffs and key system - parameters. The technique is applied to real electrocardiogram (ECG) - data with results that indicate the potential usefulness of the method - for heartbeat wave location and/or ECG data compression and automatic - diagnosis.

THESIS SUPERVISOR : Alan S. Willsky

TITLE : Associate Professor of Electrical Engineering.

Acknowledgements

I would like to express my deep gratitude to Prof. Alan S. Willsky, teacher and great friend, for his guidance and patience throughout this research . Dr. Don Gustafson of the Charles Stark Draper Laboratory for many discussions and useful suggestions.

This research was conducted at the M.I.T. Electronic Systems Laboratory, with partial support provided by NASA Ames Research Center under Grant No. NGL-22-009-124 and at the Charles Stark Draper Laboratory with support --- from the U.S. Air Force School of Aerospace Medicine under contract No. F41609-76-C-0009.

To Loli :

For the beautiful moments we have spent together and our ilusion of wonderful years to come

To my brother Joaquin and to the great memory of my younger brother Juan Carlos

To my wonderful parents :

For their advice and their help

To my country , Mexico

TABLE OF CONTENTS

Chapter I

Introduction and Motivation

I.1) Spline Approximation Problem

Throughout the years, a great deal of work has been devoted to determine an automatic diagnoses system using electrocardiogram (ECG) data.[8,9] In this research work we will try to determine the feasibility of using polynomial approximation over variable segments of ECG's. Specifically , our approach will consider spline functions [1,2] for electrocardiogram modeling. There are several reasons for doing this :

a) Since the amount of data generated by ECG's is enormous, polynomial approximation may allow data compression.

b) Spline functions provide the location of knots, which may have diag-- nostic significance. For example, the knot location may tell us when certain cardiac events occur.

The approximation problem can be visualized as in Fig. I.1.

Consider subdividing the fixed time interval $T_0 < t < T_N$ of ECG data into N subregions delimited by the mesh of knots :

$$\theta : \quad T_0 < T_1 < \ldots < T_N$$

The ECG model is a function $S_\theta(y,t)$ constrained to match exactly the a---

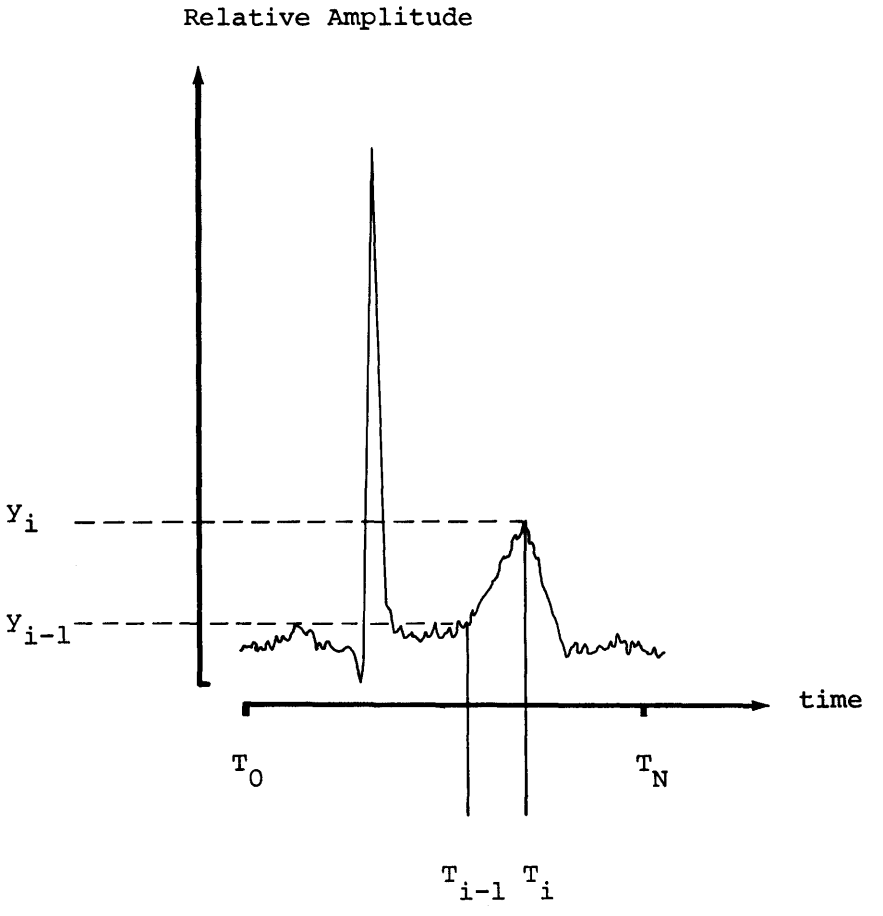

Fig. I.1

ssociated set of ordinates y_i prescribed :

$$Y : \quad y_0 , y_1 , y_2 , \cdots , y_N$$

Within each interval between the knots, ECG data y(t) is approximated by a finite (n-1)st order polynomial, whose unknown coefficients must be determined. Usually, a convenient constraint imposed on the approxima-- ting (n-1)st order polynomials is to require $S_\theta(y,t)$ to be continuous

together with its first, second, ... (n-2)nd derivatives on $T_0 < t < T_N$.
In the literature, this condition is given the name " Maximum Smoothness "
The parameters of the spline function $S_\theta(y,t)$ will consequently be :

1) the location of the " optimal knots ", and
2) the coefficients of the (n-1)st order polynomials used in the ---- approximation between knots.

I.2) Failure Detection Problem

In the past few years, a great deal of research in system theory has been directed to the problem of the detection of abrupt changes in dynamical systems. In this paper, such changes will be referred to as " failures ", although such changes may have quite different physical mea---- nings.
Much of the failure detection analysis has been performed in the context of a state space description of a linear dynamical system as follows :

State Equation

$$x(k+1) = \Phi(k)x(k) + B(k)u(k) + w(k) \qquad (I.2.1)$$

Sensor Equation

$$z(k) = H(k)x(k) + J(k)u(k) + v(k) \qquad (I.2.2)$$

where : u(k) is a known input ; w(k) and v(k) are independent, zero ---- mean, white Gaussian sequences with covariance matrices Q and R respectively.

Recent studies have provided different approaches to the failure detec-- tion problem. Among them, the generalized likelihood ratio (GLR) technique, first suggested by A.S.Willsky and H.Jones [6] has been widely studied and successfully applied to a variety of practical problems [3]. Moreover, the GLR technique provides an estimate of the failure magnitude and the time of occurrence of the failure which are important in some applications. We present a brief description of the GLR method in Chapter II.

Thus far, we have considered the spline approximation problem and the --- failure detection problem independently. Now we can raise the following question : Is it possible to use the GLR detection approach to identify the " optimal knot " location for spline functions, and can this approach be useful in processing ECG's ? The goal of this research is the thorough investigation of this question.

I.3) The Spline Model

The essence of our dynamic model is captured by the knot location problem. The basic point of departure for constructing a dynamical system is the -

" Maximum Smoothness " property of splines.

Given an (n-1)st order polynomial y(t) define :

$$\begin{aligned} y(t) &= x_1(t) \\ \dot{y}(t) &= x_2(t) \\ &\vdots \quad\quad \vdots \\ y^{(n-1)}(t) &= x_n(t) \end{aligned} \tag{I.3.1}$$

and

$$x(t) = \begin{bmatrix} x_1(t) \\ x_2(t) \\ \vdots \\ x_n(t) \end{bmatrix} \tag{I.3.2}$$

Suppose now that y(t) is actually an (n-1)st order spline -i.e. it is piecewise an (n-1)st order polynomial with discontinuities in the ---- highest derivative at the knot times [T_i]. We then have the dynamical equation for x(t) :

$$\dot{x}(t) = A\,x(t) + F_n\,\alpha\,\delta(t-T_{i-1}) \tag{I.3.3}$$

$$T_{i-2} < t < T_i$$

$$y(t) = H\, x(t) \qquad \text{(I.3.4)}$$

where :

$$A = \begin{bmatrix} 0 & 1 & 0 & 0 & \dots & 0 \\ 0 & 0 & 1 & 0 & \dots & 0 \\ 0 & 0 & 0 & 1 & \dots & 0 \\ \vdots & & & & \ddots & \\ 0 & 0 & 0 & 0 & \dots & 1 \\ 0 & 0 & 0 & 0 & \dots & 0 \end{bmatrix} \qquad F_n = \begin{bmatrix} 0 \\ 0 \\ 0 \\ \vdots \\ 0 \\ 1 \end{bmatrix} \qquad H^T = \begin{bmatrix} 1 \\ 0 \\ 0 \\ \vdots \\ 0 \\ 0 \end{bmatrix}$$

and α is the magnitude of the discontinuity at $t = T_{i-1}$.

This point of view considers the spline as a dynamic system driven by impulses, much as cardiac activity is driven by a series of impulses. As our aim is to approximate ECG's by splines, a crucial question is the location of the knots -i.e. the times [T_i]. The basic premise here is that the spline approximations can be useful in allowing data compression of the ECG (without loss of diagnostic information) and that the knot locations themselves may provide information concerning the timing of cardiac events.

Discretization in Time

Upon discretizing the time invariant dynamic system, we arrive to the -- following set of equations for an (n-1)st order spline (which has an n^{th} order state representation) :

State Equation

$$x(k+1) = e^{A\Delta}\, x(k) + F_n\, \alpha\, \delta(k+1,\theta) \qquad \text{(I.3.5)}$$

Sensor Equation

$$z(k) = H\, x(k) \qquad \text{(I.3.6)}$$

where :

$$e^{A\Delta} = \begin{bmatrix} 1 & \Delta & \cdots & \Delta^{n-1}/(n-1)! \\ 0 & 1 & \cdots & \vdots \\ 0 & 0 & 1 & \vdots \\ \vdots & & \ddots & \Delta \\ 0 & 0 & 0 & 1 \end{bmatrix} \qquad \text{(I.3.7)}$$

and Δ is the time interval.

I.4) Overview of the Research

This research comprises two basic parts, analytical work and experimental

research.

a) Analytical Work

The failure detection analysis will be performed in the context of a ---- state space description of a spline. Initially, our attention will be devoted to understanding how well the GLR detection scheme can locate the knots of a spline function when we actually observe a spline in additive Gaussian noise.

In Chapter II we first introduce the basic GLR approach.There we define the likelihood ratio random variable $l(\mathbf{k},\theta)$ and derive some of its statistical properties. These expressions may be simplified using the ----- " Maximum Smoothness " property of variable knot spline functions together with the constrained GLR (CGLR) detection scheme. This simplification is used throughout our work.

In Chapter III we first present some basic results for the single knot location problem. Results include computation of the noncentrality parameter $\delta^2(k,\theta,\theta_T)$ for different order spline functions (linear, quadratic and cubic splines) . Development of equations for the multiple knot location problem is followed through and results for the two knot location problem for linear splines are presented.

In Chapter IV we derive the important sensitivity equations for the noncentrality parameter $\delta^2(k,\theta,\theta_T)$ in an attempt to obtain a more precise

knowledge of its behavior as a function of some important input parame---ters, i.e. the sensor noise covariance R and the elements of the error -- covariance matrix P(0/0).

In Chapter V we also introduce the useful concept of " age-weighting " filtering, which allows the GLR detector to be more sensitive to new in--formation. Results for several age-weighting time constants for the sin--gle knot and the two knot location problem are presented for the linear spline case.

b) Experimental Research

Our analytical work provides us with an understanding of GLR performance in locating knots when one actually observes a spline in additive Gaussian noise. In Chapter VI we analyze how well the CGLR knot location system works when we in fact approximate waveforms that are NOT splines, specifi-cally ECG's.

The goal of this effort is to determine the feasibility of using such an approach for data compression and/or as part of an automatic diagnosis system.

Chapter II

Generalized Likelihood Ratio Approach

II.1) Description of the GLR Technique

The GLR detection system assumes :

a) a discrete time linear dynamical system of the form :

State Equation

$$x(k+1) = e^{A\Delta}\, x(k) + \delta(k+1,\theta)\, \upsilon + w(k) \qquad \text{(II.1.1)}$$

Sensor Equation

$$z(k) = H(k)\, x(k) + v(k) \qquad \text{(II.1.2)}$$

where : $x(k) \in R^n$ represents the state with Gaussian initial condition $x(0)$, mean $\bar{x}(0)$ and covariance $P(0/0)$. In addition $w(k)$ and $v(k)$ are independent, zero mean, white Gaussian random sequences with covariance matrices Q and R respectively. In this problem $e^{A\Delta}$ is a constant as given by equation (I.3.7) ; Δ represents the time interval (for this project, Δ has been chosen as 4 msec.) ; θ is the failure time - an unknown positive integer which assumes a finite value if a jump occurs and takes the value ∞ if there is no jump. Also δ_{ij} is the Kronecker delta, and υ is the un---- known failure.

and

b) a Kalman-Bucy filter (that assumes no failure $\theta = \infty$) characterized by the following equations [7] :

State Estimate Extrapolation

$$\hat{x}(k/k-1) = e^{A\Delta}\, \hat{x}(k-1/k-1) \qquad \text{(II.1.3)}$$

State Estimate Update

$$\hat{x}(k/k) = \hat{x}(k/k-1) + K(k)\, \gamma(k) \qquad \text{(II.1.4)}$$

Innovation Process

$$\gamma(k) = z(k) - H\, \hat{x}(k/k-1) \qquad \text{(II.1.5)}$$

where : $\gamma(k)$ is a zero mean , white Gaussian residual with covariance matrix $V(k)$. $K(k)$ is known as the Kalman filter gain, computed recursively as follows :

Error Covariance Update Matrix

$$P(k-1/k-1) = (I - K(k-1)\, H)\, P(k-1/k-2) \qquad \text{(II.1.6)}$$

Error Covariance Extrapolation Matrix

$$P(k/k-1) = e^{A\Delta}\, P(k-1/k-1)\, (e^{A\Delta})^{T} + Q \qquad \text{(II.1.7)}$$

Residual's Covariance Matrix

$$V(k) = H\, P(k/k-1)\, H^{T} + R \qquad \text{(II.1.8)}$$

Kalman Filter Gain

$$K(k) = P(k/k-1)\, H^{T}\, V^{-1}(k) \qquad \text{(II.1.9)}$$

Schematically, the GLR detection scheme is presented in Fig. II.1.

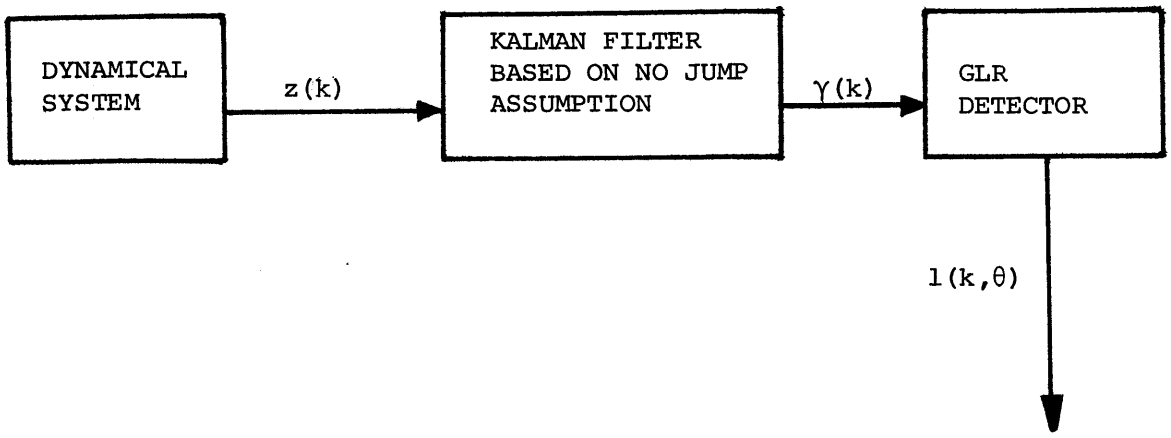

Fig. II.1

Due to the linearity of the system and filter, the residuals $\gamma(k)$ can be written as :

$$\gamma(k) = \gamma_I(k) + \gamma_{II}(k) \qquad \text{(II.1.10)}$$

where : $\gamma_I(k)$ corresponds to all effects except θ (failure time) and υ (magnitude and direction of the failure).

$\gamma_{II}(k)$ corresponds to the effects of θ and υ .

The above equation can be written as :

$$\gamma(k) = \gamma_I(k) + G(k,\theta)\upsilon \qquad \text{(II.1.11)}$$

where : $G(k,\theta)$ is a matrix called the " failure signature " matrix and characterizes the way in which a failure υ at time θ propagates through the system and affects the residual $\gamma(k)$ at time k. A computational algorithm for $G(k,\theta)$ can be based upon the following equations [6] :

$$G(k,\theta) = H[\ (e^{A\Delta})^{k-\theta} - e^{A\Delta}\ F(k-1,\theta)\ ] \qquad \text{(II.1.12)}$$

$$F(k,\theta) = K(k)\ G(k,\theta) + e^{A\Delta}\ F(k-1,\theta) \qquad \text{(II.1.13)}$$

The only new additional equation is for a jump at the present time k :

$$F(k,k) = K(k)*H \qquad \text{(II.1.14)}$$

We can establish two hypotheses :

H_0 : no failure has occurred

H_1 : a failure has occurred

Using the fact that the residuals $\gamma(k)$ are independent and Gaussian, we obtain the following expressions : let

$$\Lambda(k,\ ) = \frac{f(\ \gamma(1),\ldots,\ \gamma(k)/\ H_1,\ \theta\ ,\ \hat{\upsilon}(k,\theta))}{f(\ \gamma(1),\ldots,\ \gamma(k)/\ H_0)} \qquad \text{(II.1.15)}$$

where : $\hat{\upsilon}(k,\theta)$ is the best estimate of υ assuming a failure at time θ , and f is the density function for the residuals $\gamma(k)$ given the corresponding information. Also let

$$l(k,\theta) = 2 \ln \Lambda(k,\theta) \qquad \text{(II.1.16)}$$

and define :

$$d(k,\theta) = \sum_{j=1}^{k} G^T(j,\theta)\, V^{-1}(j)\, \gamma(j) \qquad \text{(II.1.17)}$$

and the information matrix

$$C(k,\theta) = \sum_{j=1}^{k} G^T(j,\theta)\, V^{-1}(j)\, G(j,\theta) \qquad \text{(II.1.18)}$$

Then we have [6] :

Likelihood Ratio

$$l(k,\theta) = d^T(k,\theta)\, C^{-1}(k,\theta)\, d(k,\theta) \qquad \text{(II.1.19)}$$

Maximum Likelihood Estimates (MLE)

$$\hat{\upsilon}(k,\theta) = C^{-1}(k,\theta)\, d(k,\theta) \qquad \text{(II.1.20)}$$

$$\hat{\theta}(k) = \text{ARG MAX } l(k,\theta) \qquad \text{(II.1.21)}$$

$$\theta \in \textcircled{H}\ (k)$$

$$\hat{\upsilon}(k) = \hat{\upsilon}(k,\hat{\theta}(k)) \qquad \text{(II.1.22)}$$

Here Ⓗ (k) is the set of postulated failure times considered at time k. As indicated in [6], a computationally appealing choice is the --- singleton set Ⓗ (k) = [k-N] for some N.

II.2) Constrained Generalized Likelihood Ratio (CGLR)

We now cosider the case in which we assume $\upsilon = \alpha F_n$. Following [6] we have :

MLE of α

$$\hat{\alpha}(k,\theta) = F_n^T d(k,\theta) \; / \; F_n^T C(k,\theta) F_n \qquad \text{(II.2.1)}$$

Likelihood Ratio

$$l(k,\theta) = [F_n^T d(k,\theta)]^2 \; / \; F_n^T C(k,\theta) F_n \qquad \text{(II.2.2)}$$

Finally, the MLE of $\hat{\theta}(k)$ is the value $\theta < k$ that maximizes the above ex-- pression. Then our decision rule is :

$$l(k,\hat{\theta}) \underset{H_0}{\overset{H_1}{\gtrless}} \varepsilon \qquad \text{(II.2.3)}$$

The implementation of the GLR detector involves a growing number of filters [6] . To avoid tis problem we can restrict our attention to a " sliding window " of finite width -i.e. Ⓗ (k) = [k-N,k-N+1,...,k-M].

II.3) Statistical Properties of $l(k,\Theta)$

Suppose a jump of size υ actually occurs at time Θ_T. Given this infor-- mation, $d(k,\Theta)$ is Gaussian and its statistics can be calculated. A ----- straightforward computation yields :

$$E\ [\ d(k,\theta)\ ] = \sum_{j=MAX(\Theta,\Theta_T)}^{k} G^T(j,\theta)\ V^{-1}(j)\ G(j,\theta_T)\ F_n\ \alpha$$

$$E\ [\ d(k,\theta)\ ] = C(k,\theta,\theta_T)\ F_n\alpha$$

$$COVAR\ [\ d(k,\theta)\ ] = C(k,\theta) \qquad \text{(II.3.1)}$$

Thus, $l(k,\theta)$ is the square of a Gaussian random variable - i.e. it is a noncentral χ^2 random variable with one degree of freedom and :

$$E\ [\ l(k,\theta)\ ] = E\ [\ (\ F_n^T\ d(k,\theta))^2\ ]/\ F_n^T\ d(k,\theta)\ F_n \qquad \text{(II.3.2)}$$

$$E\ [\ l(k,\theta)\ ] = 1 + \delta^2(k,\theta,\theta_T)$$

Here δ^2 is the noncentrality parameter whose value is given by :

$$\delta^2(k,\theta,\theta_T) = \alpha^2\ [\ F_n^T\ C(k,\theta,\theta_T)\ F_n\ ]^2\ /\ F_n^T\ C(k,\theta)\ F_n \qquad \text{(II.3.3)}$$

Chapter III

Knot Location Problem

III.1) Single Knot Location

In the previous chapter we have derived some properties of the CGLR ---- failure detection system for the single knot location problem (only one real failure at time θ_T), by studying some statistical properties of the likelihood ratio random variable $l(k,\theta)$.

As pointed out, the implementation of the CGLR detector involves maximizing the likelihood ratio expression (II.2.2). This last statement leads us to expect maximum values of the likelihood ratio $l(k,\theta)$ for maximum - values of the noncentrality parameter $\delta^2(k,\theta,\theta_T)$. We would expect the -- largest value for $\theta = \theta_T$, and the rate at which δ^2 decreases as we change - tells us how well GLR can isolate the knot location.

In order to get some practical insight into the nature of the CGLR detection scheme we have developed a FORTRAN computer program for computing --the noncentrality parameter $\delta^2(k,\theta,\theta_T)$. The flow -chart for this program is presented in Fig. III.1.

Computation of $\delta^2(k,\theta,\theta_T)$ has been performed for linear, quadratic and -- cubic splines for several sets of values for the input parameters R (sensor's noise covariance) and P(o/o) (error covariance matrix).

In Fig.III.2 to III.13 we have plotted the noncentrality parameter δ^2 in

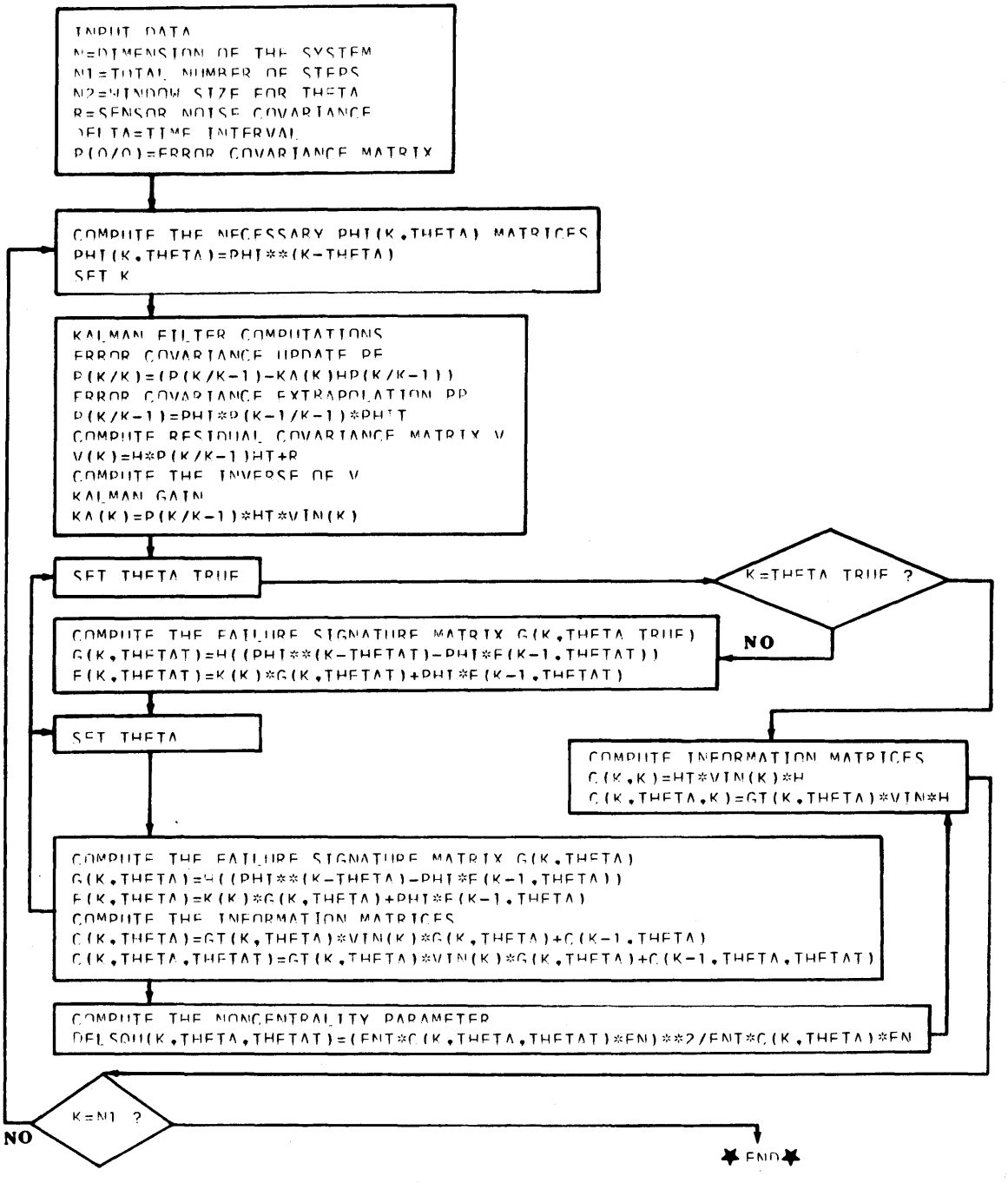
INPUT DATA
N=DIMENSION OF THE SYSTEM
N1=TOTAL NUMBER OF STEPS
N2=WINDOW SIZE FOR THETA
R=SENSOR NOISE COVARIANCE
DELTA=TIME INTERVAL
P(0/0)=ERROR COVARIANCE MATRIX
COMPUTE THE NECESSARY PHI(K,THETA) MATRICES
PHI(K,THETA)=PHI**(K-THETA)
SET K
KALMAN FILTER COMPUTATIONS
ERROR COVARIANCE UPDATE PP
P(K/K)=(P(K/K-1)-KA(K)HP(K/K-1))
ERROR COVARIANCE EXTRAPOLATION PP
P(K/K-1)=PHI*P(K-1/K-1)*PHI'T
COMPUTE RESIDUAL COVARIANCE MATRIX V
V(K)=H*P(K/K-1)HT+R
COMPUTE THE INVERSE OF V
KALMAN GAIN
KA(K)=P(K/K-1)*HT*VIN(K)
SET THETA TRUE
K=THETA TRUE ?
NO
COMPUTE THE FAILURE SIGNATURE MATRIX G(K,THETA TRUE)
G(K,THETAT)=H((PHI**(K-THETAT)-PHI*F(K-1,THETAT))
F(K,THETAT)=K(K)*G(K,THETAT)+PHI*F(K-1,THETAT)
SET THETA
COMPUTE INFORMATION MATRICES
C(K,K)=HT*VIN(K)*H
C(K,THETA,K)=GT(K,THETA)*VIN*H
COMPUTE THE FAILURE SIGNATURE MATRIX G(K,THETA)
G(K,THETA)=H((PHI**(K-THETA)-PHI*F(K-1,THETA))
F(K,THETA)=K(K)*G(K,THETA)+PHI*F(K-1,THETA)
COMPUTE THE INFORMATION MATRICES
C(K,THETA)=GT(K,THETA)*VIN(K)*G(K,THETA)+C(K-1,THETA)
C(K,THETA,THETAT)=GT(K,THETA)*VIN(K)*G(K,THETA)+C(K-1,THETA,THETAT)
COMPUTE THE NONCENTRALITY PARAMETER
DELSQU(K,THETA,THETAT)=(ENT*C(K,THETA,THETAT)*EN)**2/ENT*C(K,THETA)*EN
K=N1 ?
NO
END

Fig.III.1

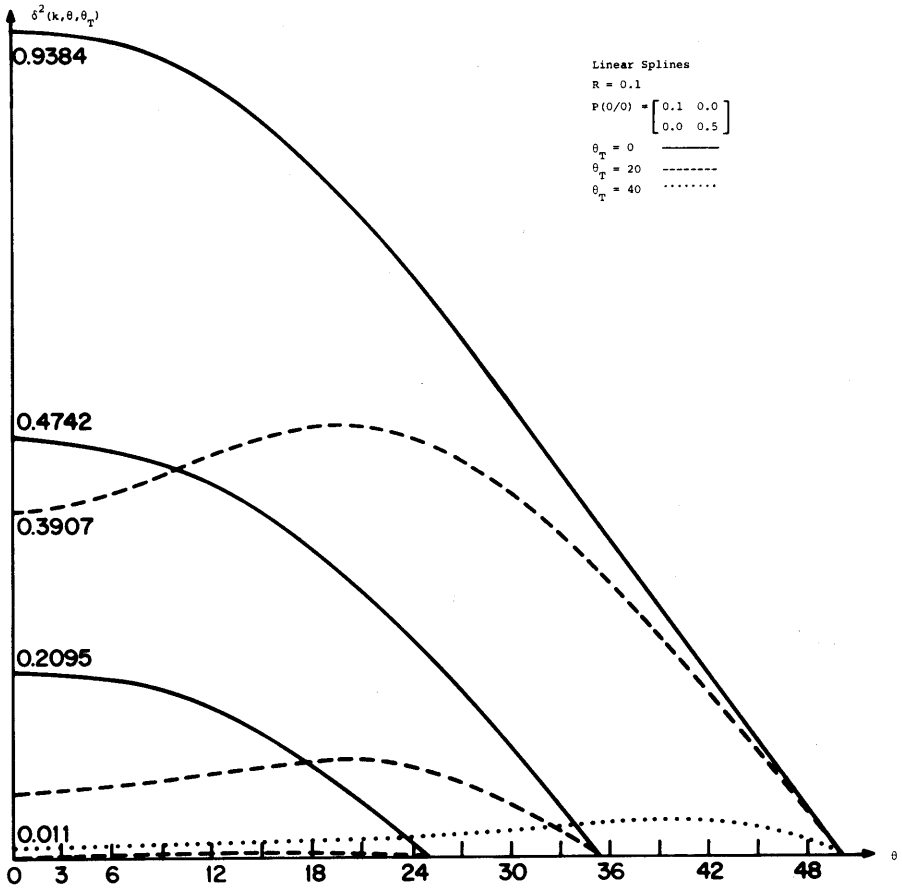
$\delta^2(k,\theta,\theta_T)$
0.9384
0.4742
0.3907
0.2095
0.011
Linear Splines
R = 0.1
P(0/0) = [0.1 0.0; 0.0 0.5]
θ_T = 0
θ_T = 20
θ_T = 40
0 3 6 12 18 24 30 36 42 48
θ

A

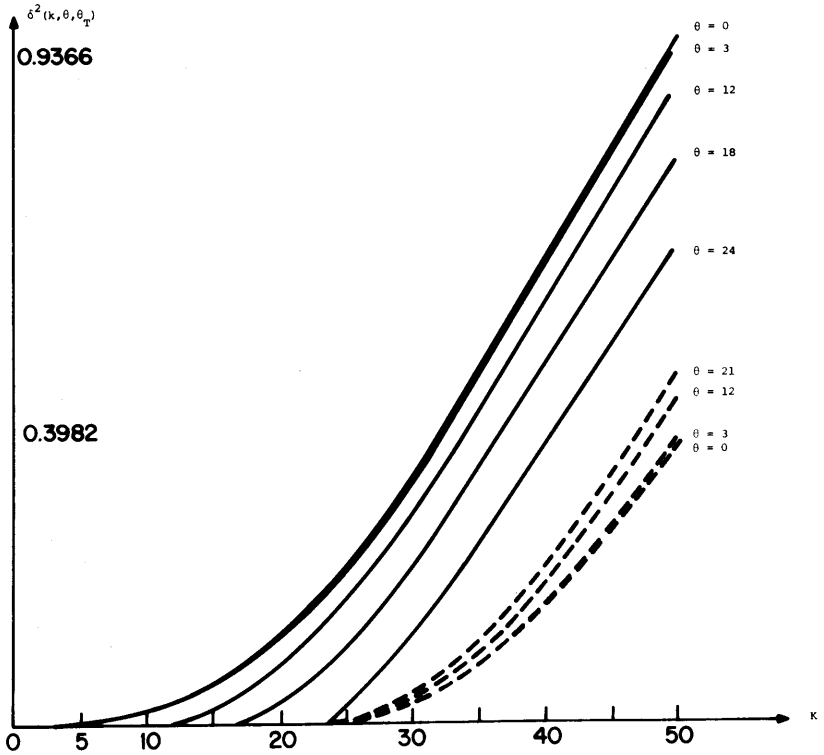
$\delta^2(k,\theta,\theta_T)$
0.9366
0.3982
θ = 0
θ = 3
θ = 12
θ = 18
θ = 24
θ = 21
θ = 12
θ = 3
θ = 0
0 5 10 20 30 40 50
K

B

Fig.III.2

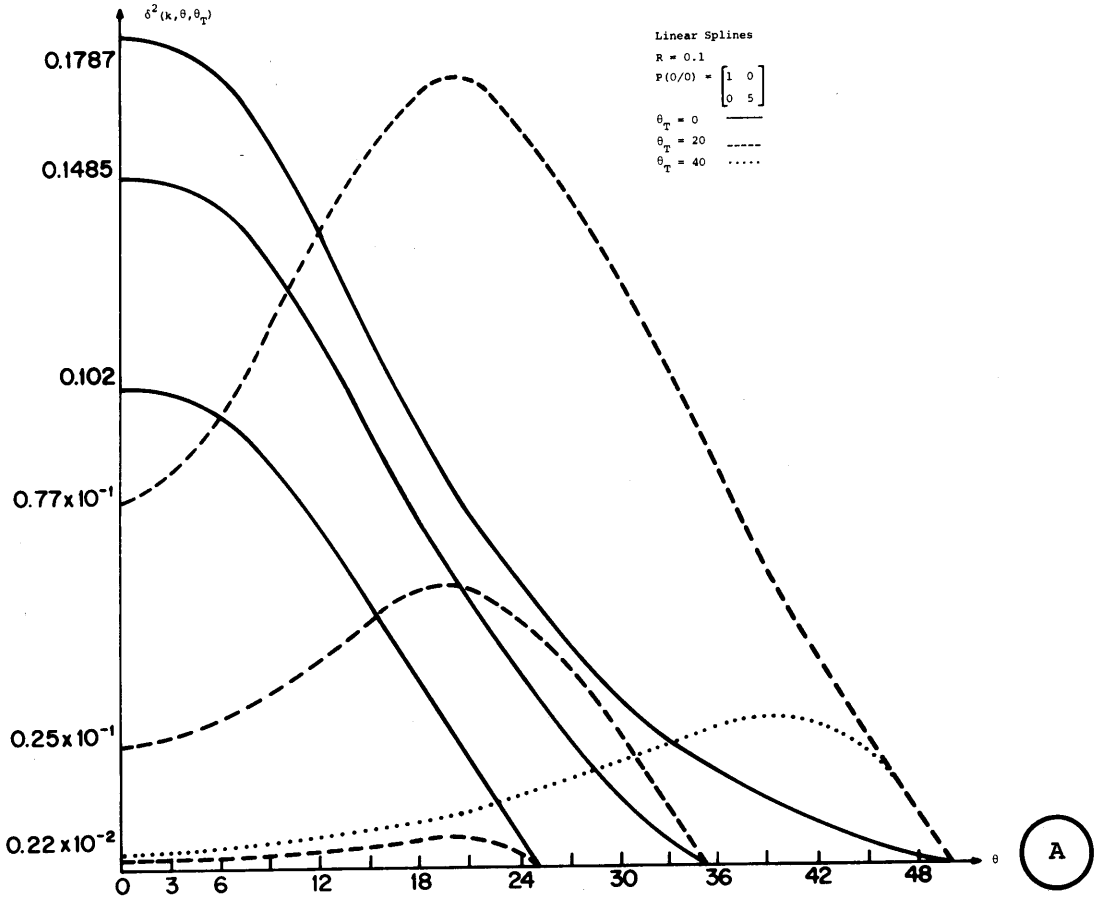
$\delta^2(k,\theta,\theta_T)$
Linear Splines
R = 0.1
P(0/0) = [1 0; 0 5]
θ_T = 0
θ_T = 20
θ_T = 40
0.1787
0.1485
0.102
0.77x10^{-1}
0.25x10^{-1}
0.22x10^{-2}
0 3 6 12 18 24 30 36 42 48
θ
A

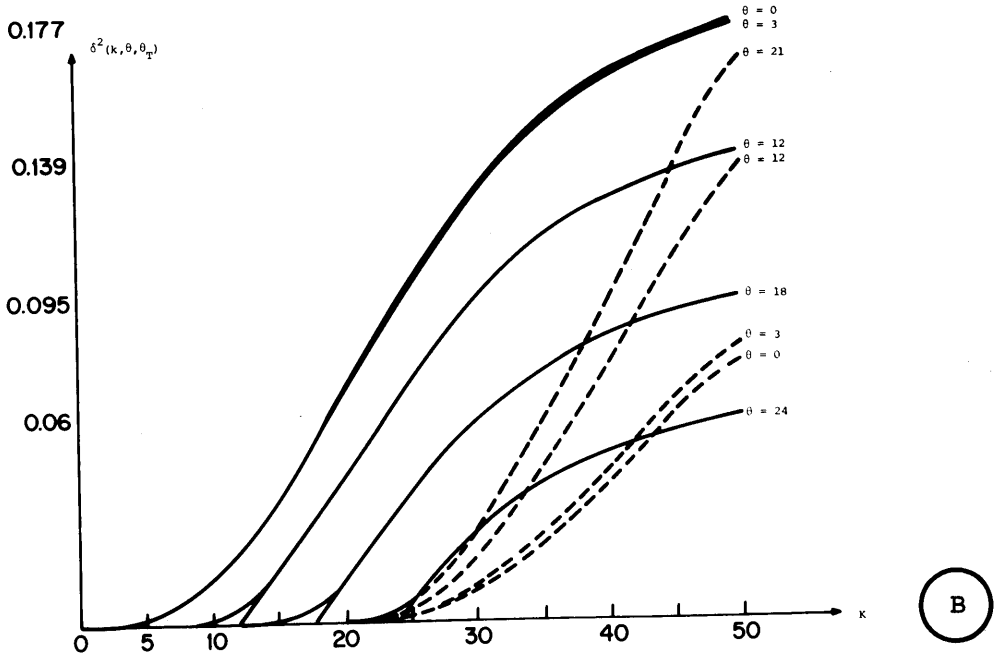
0.177
$\delta^2(k,\theta,\theta_T)$
0.139
0.095
0.06
θ = 0
θ = 3
θ = 21
θ = 12
θ = 12
θ = 18
θ = 3
θ = 0
θ = 24
0 5 10 20 30 40 50
K
B

Fig.III.3

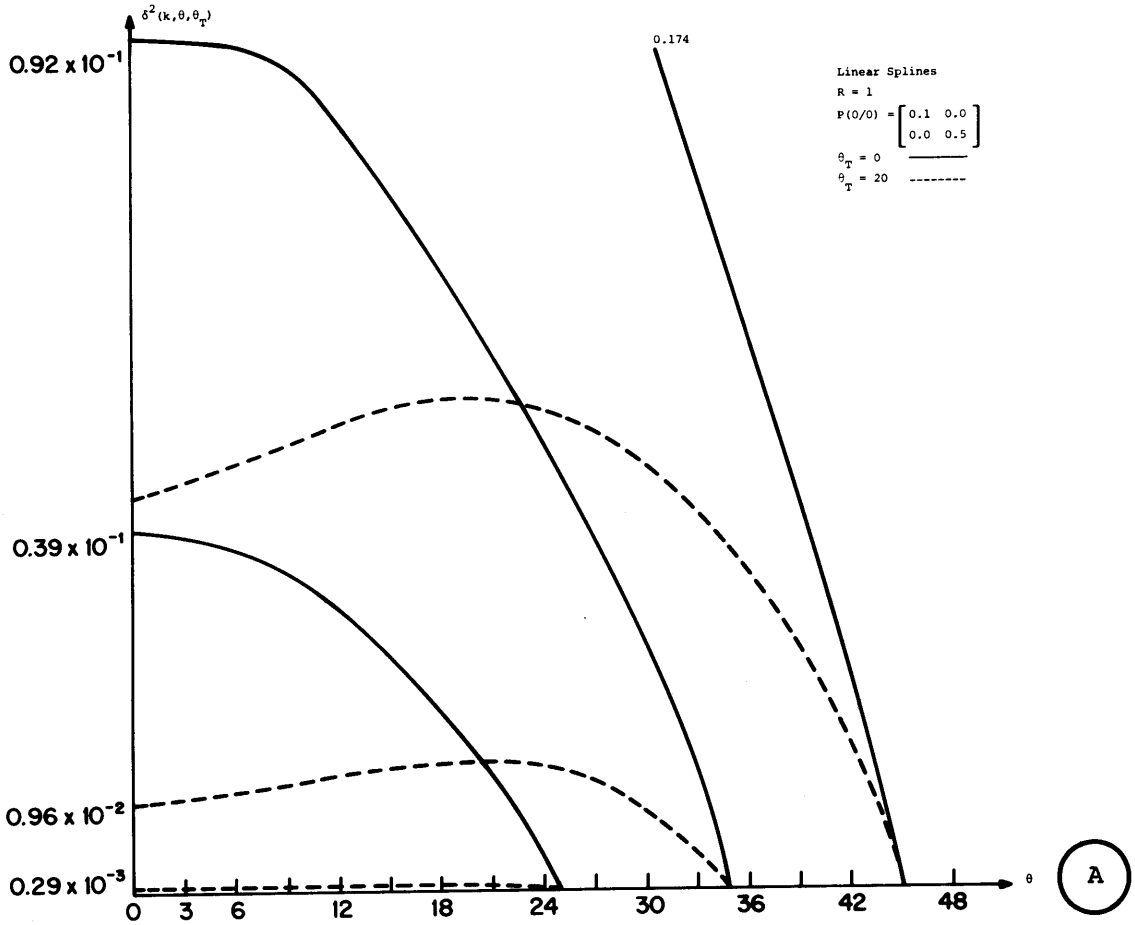
$\delta^2(k,\theta,\theta_T)$
0.92 x 10^{-1}
0.39 x 10^{-1}
0.96 x 10^{-2}
0.29 x 10^{-3}
0.174
Linear Splines
R = 1
P(0/0) = [0.1 0.0; 0.0 0.5]
θ_T = 0
θ_T = 20
0 3 6 12 18 24 30 36 42 48
θ
A

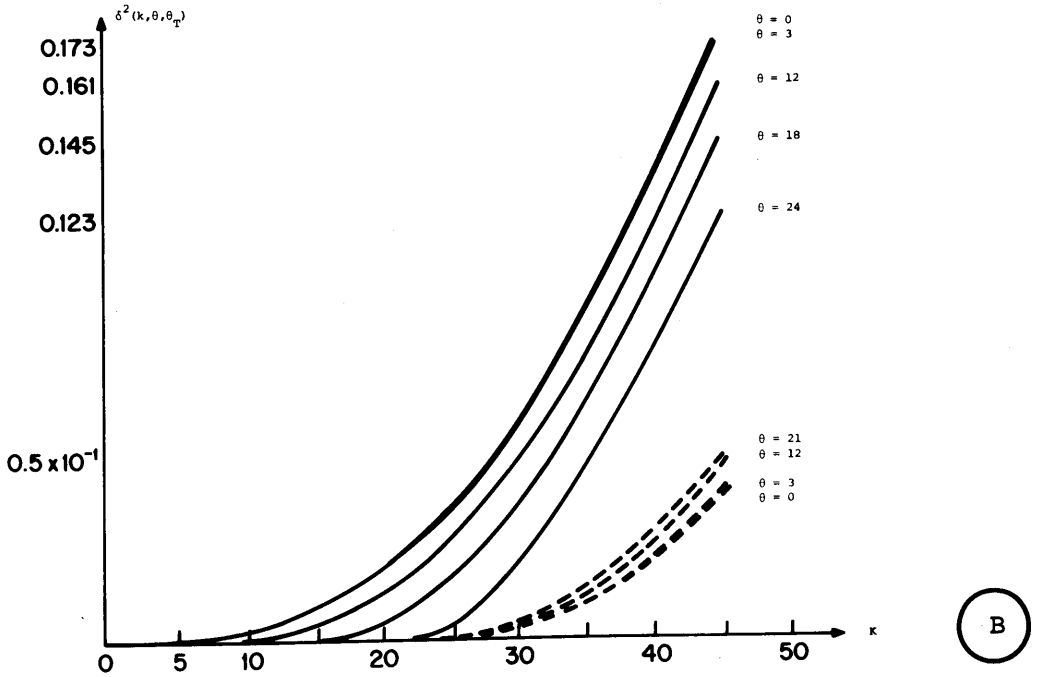
$\delta^2(k,\theta,\theta_T)$
0.173
0.161
0.145
0.123
0.5 x 10^{-1}
θ = 0
θ = 3
θ = 12
θ = 18
θ = 24
θ = 21
θ = 12
θ = 3
θ = 0
0 5 10 20 30 40 50
K
B

Fig.III.4

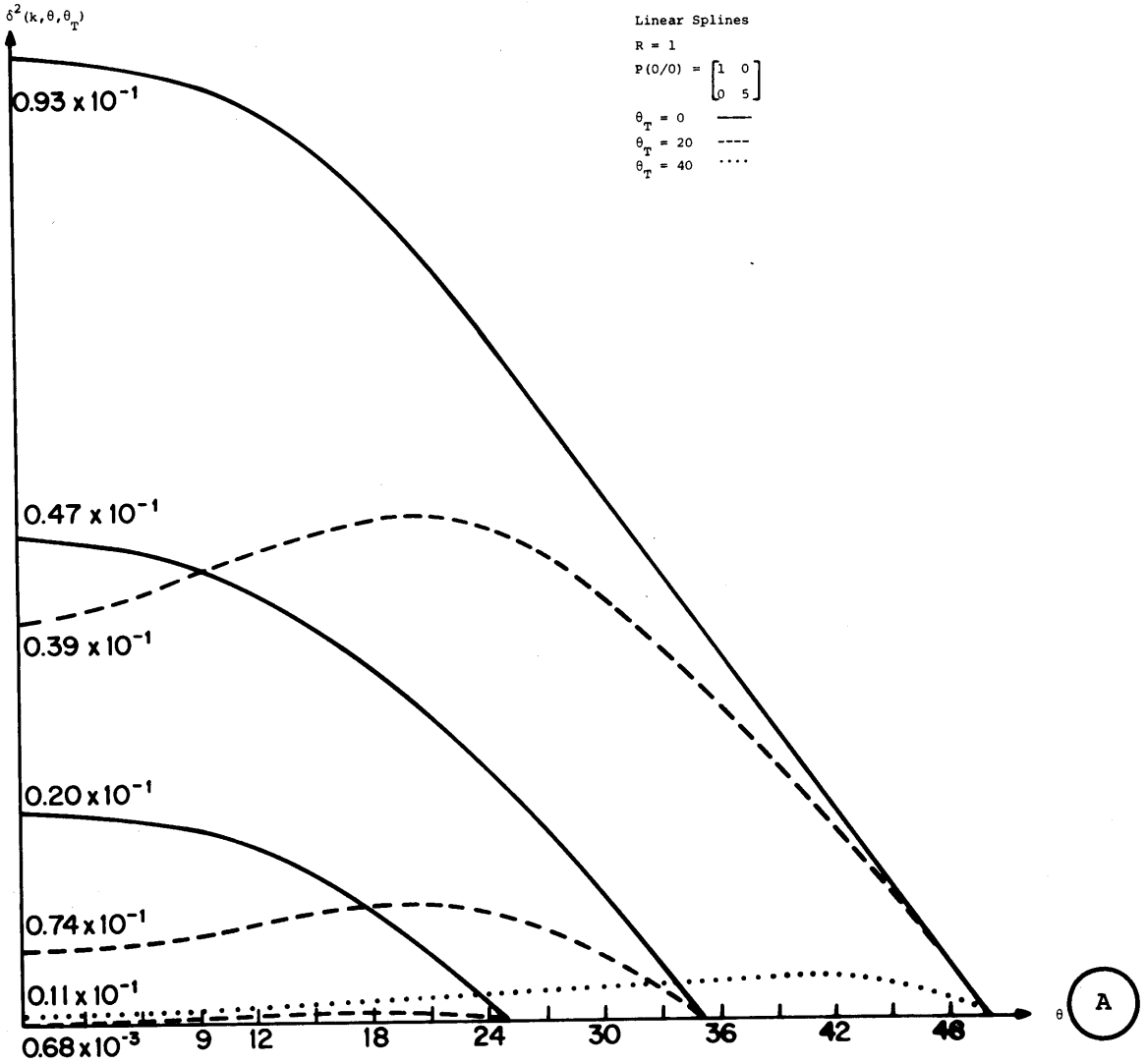
$\delta^2(k,\theta,\theta_T)$
Linear Splines
R = 1
P(0/0) = [1 0; 0 5]
θ_T = 0
θ_T = 20
θ_T = 40
0.93 x 10⁻¹
0.47 x 10⁻¹
0.39 x 10⁻¹
0.20 x 10⁻¹
0.74 x 10⁻¹
0.11 x 10⁻¹
0.68 x 10⁻³
9
12
18
24
30
36
42
48
θ
A

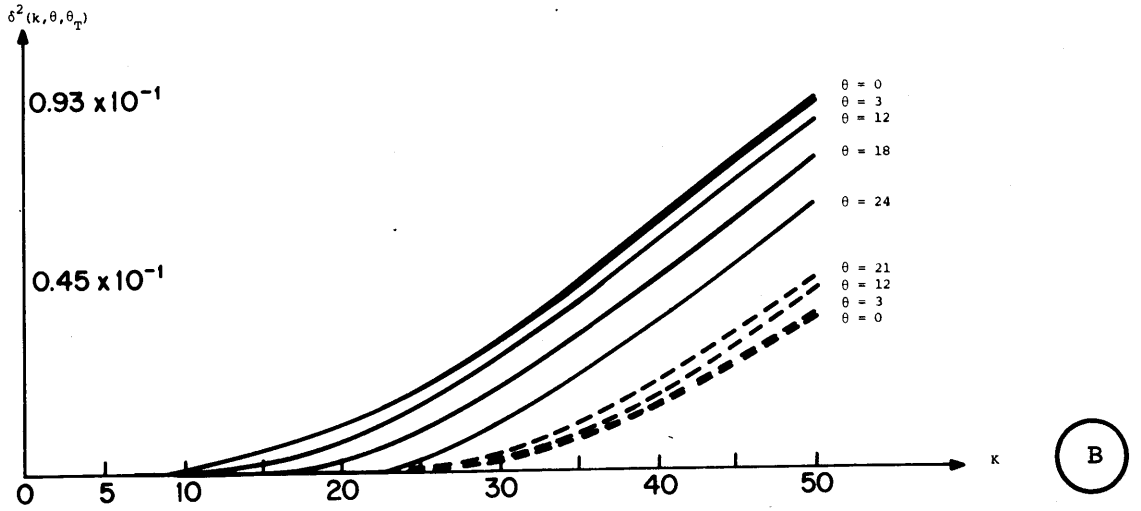
$\delta^2(k,\theta,\theta_T)$
0.93 x 10⁻¹
0.45 x 10⁻¹
θ = 0
θ = 3
θ = 12
θ = 18
θ = 24
θ = 21
θ = 12
θ = 3
θ = 0
0
5
10
20
30
40
50
K
B

Fig.III.5

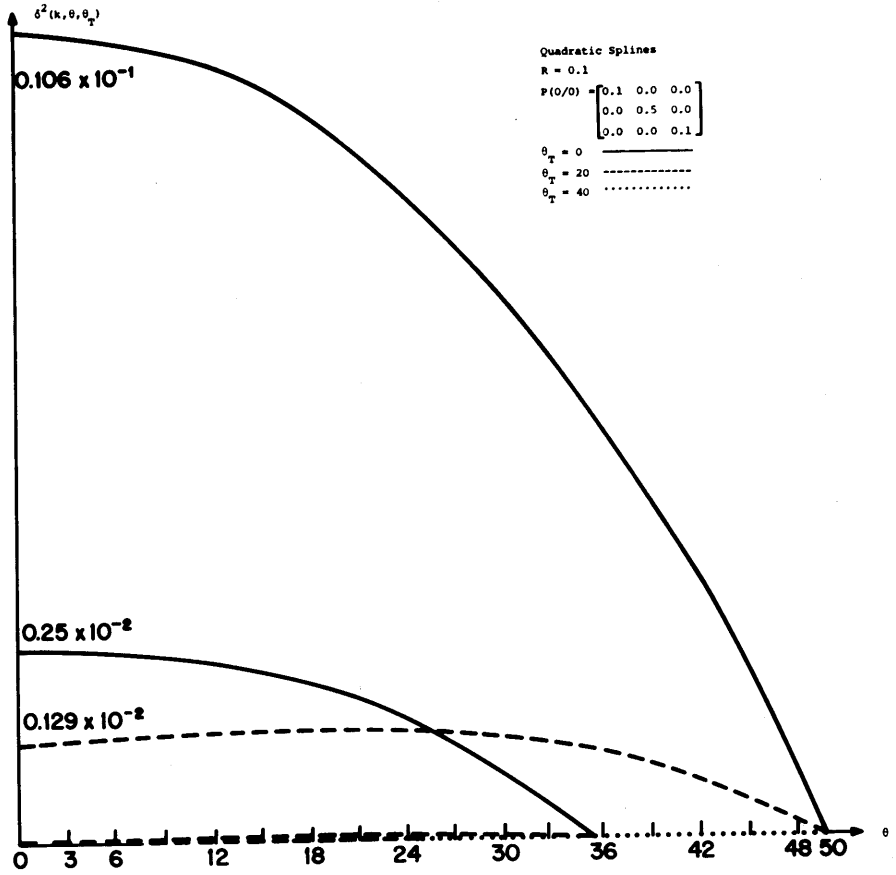
$\delta^2(k,\theta,\theta_T)$
Quadratic Splines
R = 0.1
P(0/0) = [0.1 0.0 0.0; 0.0 0.5 0.0; 0.0 0.0 0.1]
θ_T = 0
θ_T = 20
θ_T = 40
0.106 x 10^{-1}
0.25 x 10^{-2}
0.129 x 10^{-2}
0 3 6 12 18 24 30 36 42 48 50
θ

A

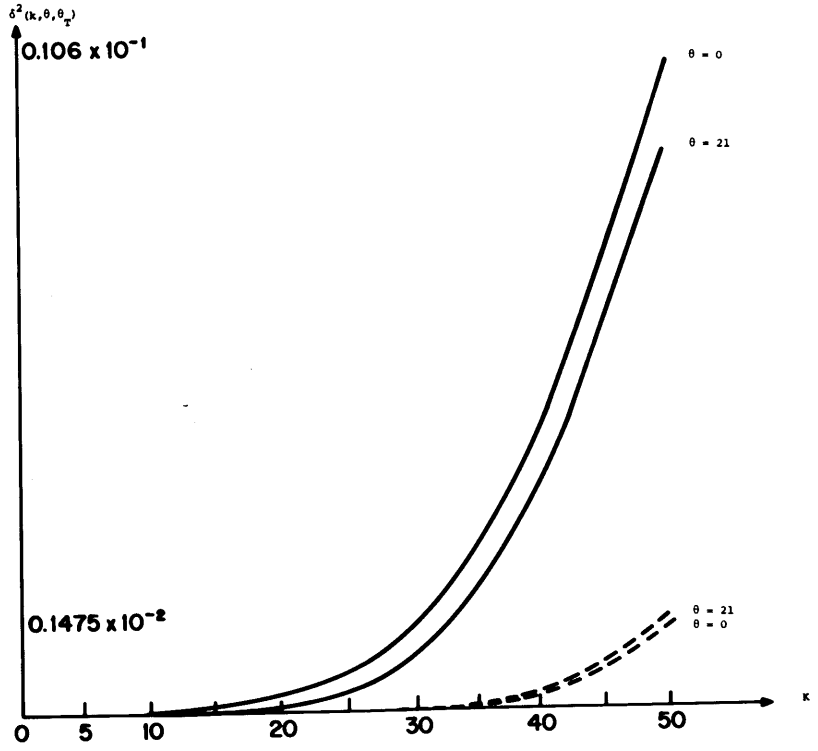
$\delta^2(k,\theta,\theta_T)$
0.106 x 10^{-1}
θ = 0
θ = 21
0.1475 x 10^{-2}
θ = 21
θ = 0
0 5 10 20 30 40 50
K

B

Fig.III.6

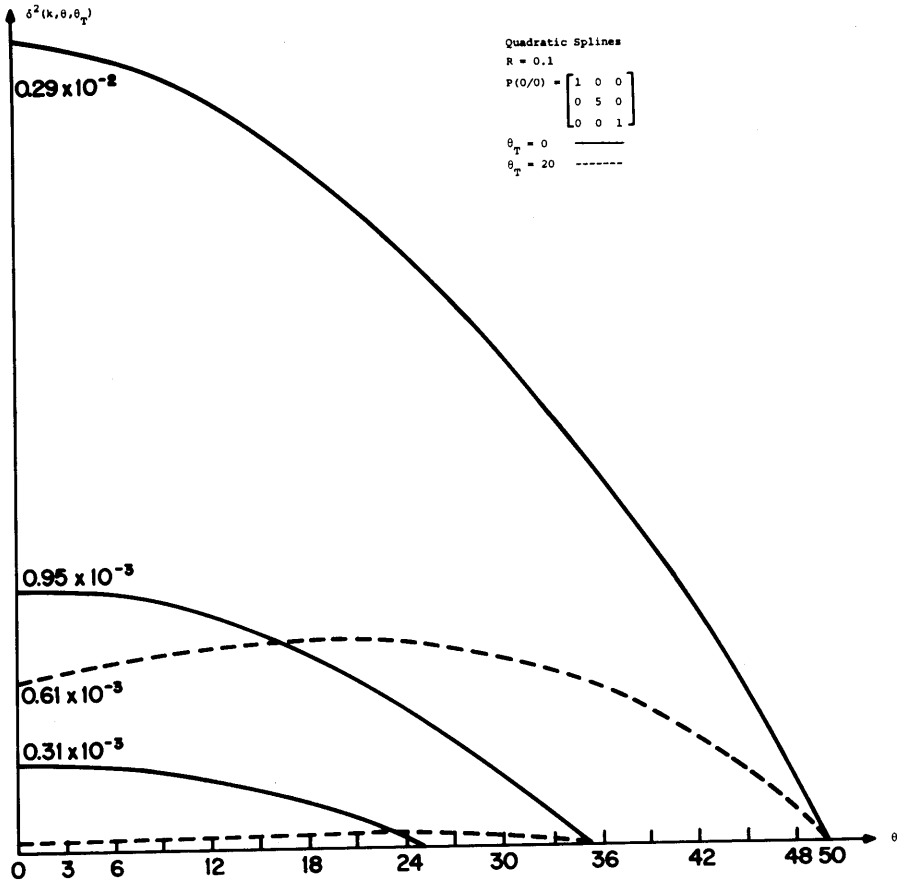
$\delta^2(k,\theta,\theta_T)$
Quadratic Splines
R = 0.1
P(0/0) = [1 0 0; 0 5 0; 0 0 1]
θ_T = 0
θ_T = 20
0.29 x 10^{-2}
0.95 x 10^{-3}
0.61 x 10^{-3}
0.31 x 10^{-3}
0 3 6 12 18 24 30 36 42 48 50
θ

A

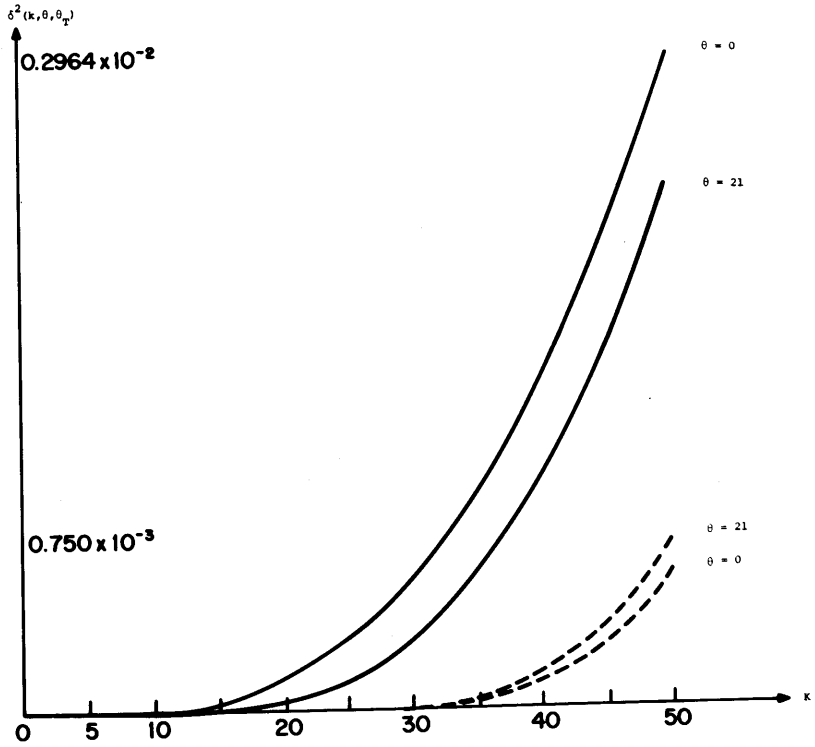
$\delta^2(k,\theta,\theta_T)$
0.2964 x 10^{-2}
0.750 x 10^{-3}
θ = 0
θ = 21
θ = 21
θ = 0
0 5 10 20 30 40 50
K

B

Fig.III.7

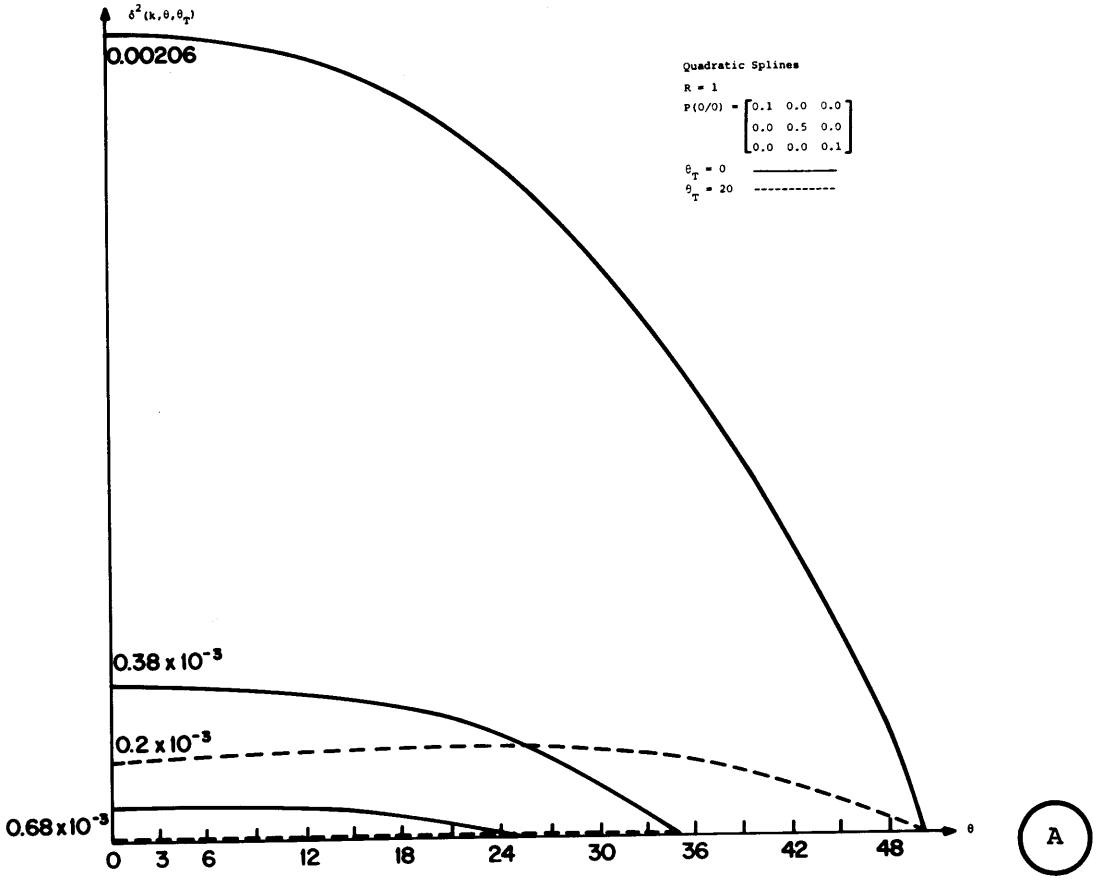
$\delta^2(k,\theta,\theta_T)$
0.00206
Quadratic Splines
R = 1
P(0/0) = [0.1 0.0 0.0; 0.0 0.5 0.0; 0.0 0.0 0.1]
θ_T = 0
θ_T = 20
0.38 x 10^{-3}
0.2 x 10^{-3}
0.68 x 10^{-3}
0 3 6 12 18 24 30 36 42 48
θ
A

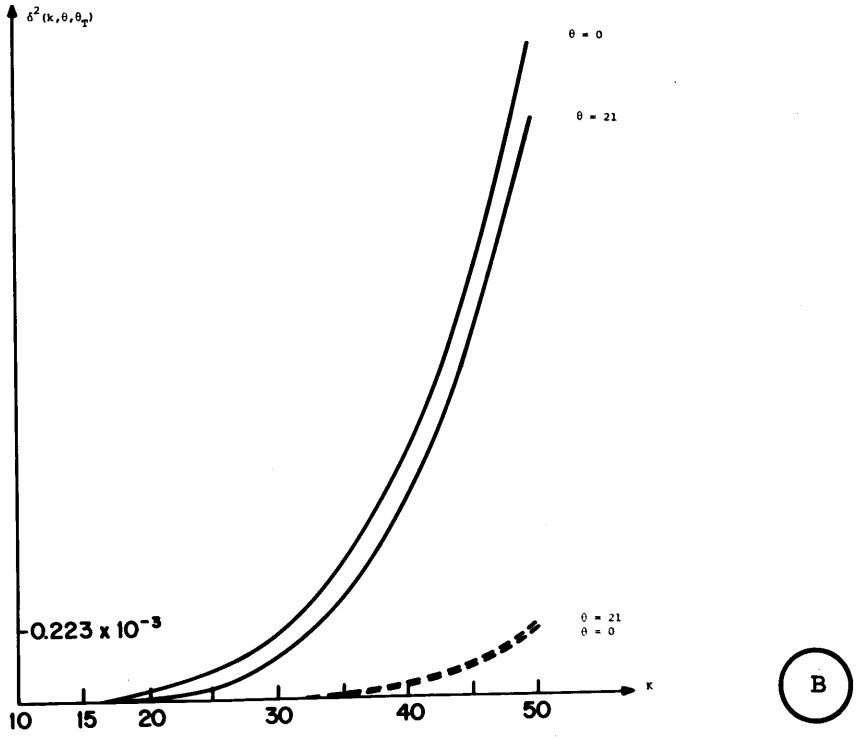
$\delta^2(k,\theta,\theta_T)$
θ = 0
θ = 21
0.223 x 10^{-3}
θ = 21
θ = 0
10 15 20 30 40 50
K
B

Fig.III.8

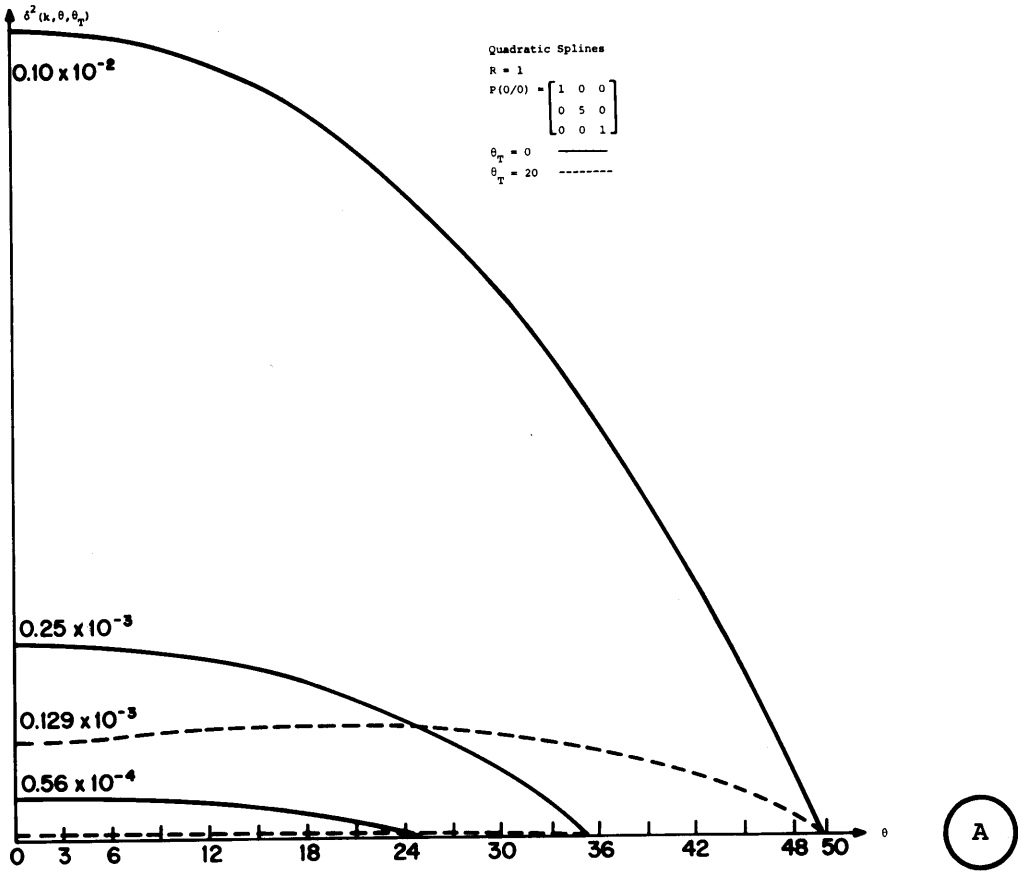
$\delta^2(k,\theta,\theta_T)$
Quadratic Splines
R = 1
P(0/0) = [1 0 0; 0 5 0; 0 0 1]
θ_T = 0
θ_T = 20
0.10 x 10^{-2}
0.25 x 10^{-3}
0.129 x 10^{-3}
0.56 x 10^{-4}
0 3 6 12 18 24 30 36 42 48 50
θ
A

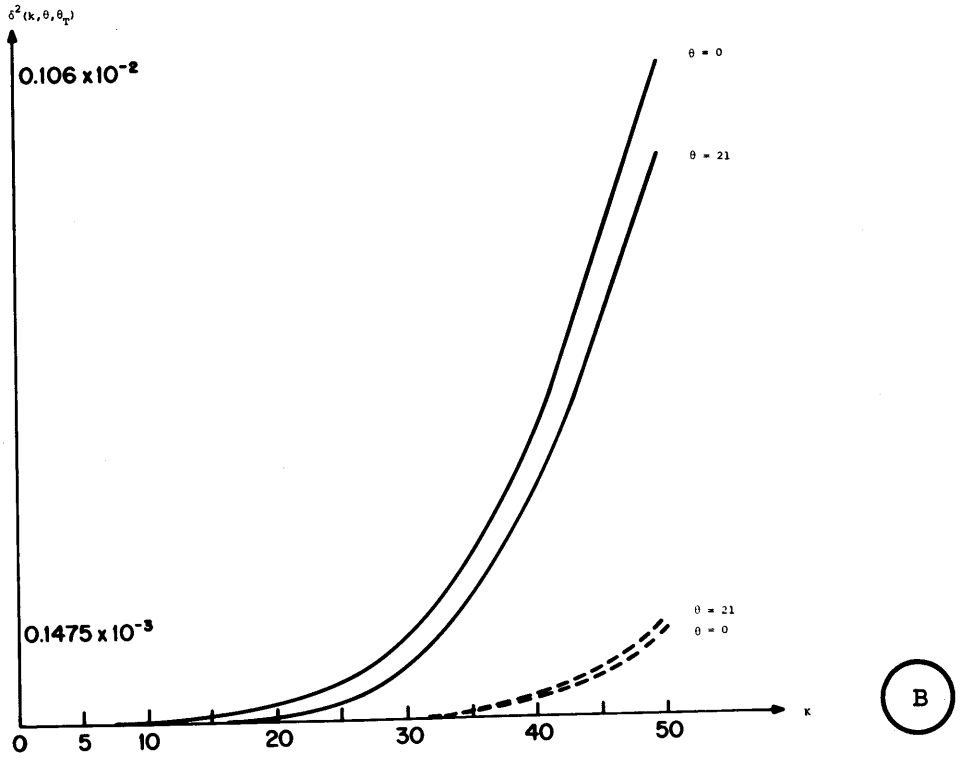
$\delta^2(k,\theta,\theta_T)$
0.106 x 10^{-2}
θ = 0
θ = 21
0.1475 x 10^{-3}
θ = 21
θ = 0
0 5 10 20 30 40 50
κ
B

Fig.III.9

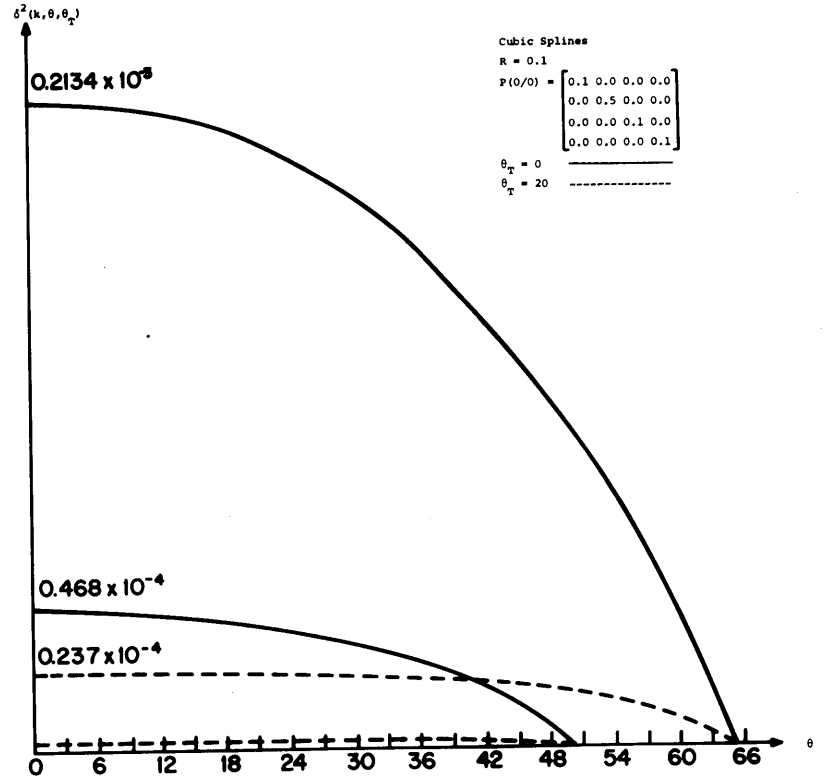
$\delta^2(k,\theta,\theta_T)$
Cubic Splines
R = 0.1
P(0/0) = [0.1 0.0 0.0 0.0; 0.0 0.5 0.0 0.0; 0.0 0.0 0.1 0.0; 0.0 0.0 0.0 0.1]
θ_T = 0
θ_T = 20
0.2134 x 10^{-3}
0.468 x 10^{-4}
0.237 x 10^{-4}
0 6 12 18 24 30 36 42 48 54 60 66
θ
A

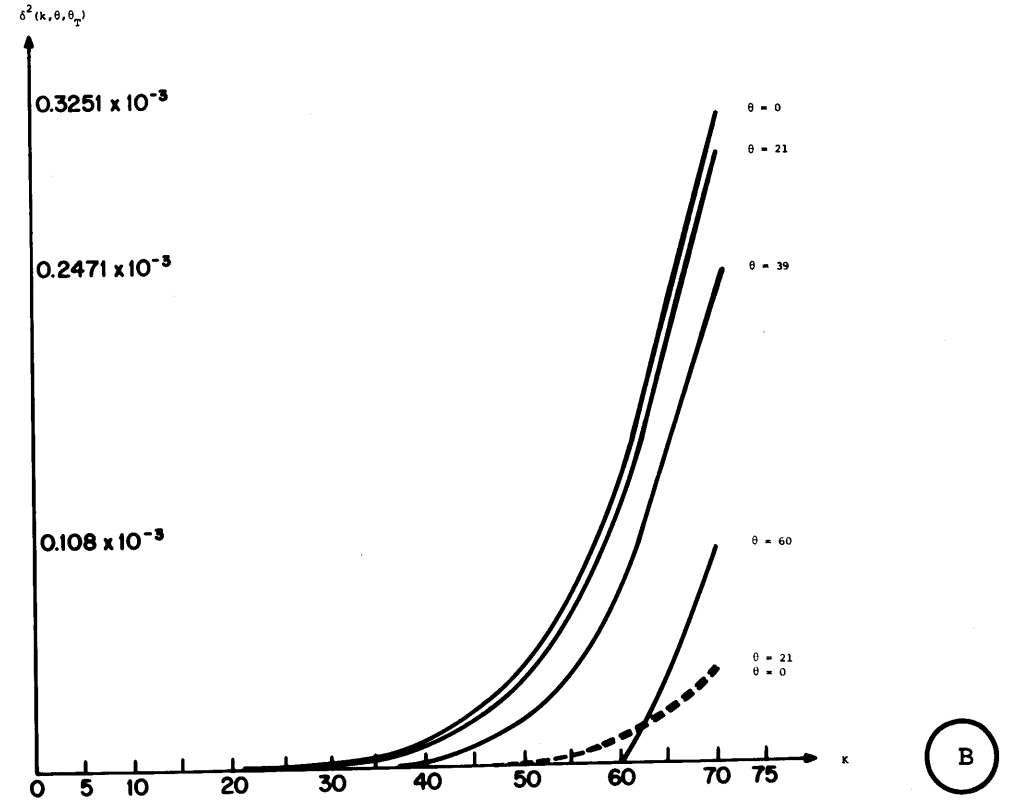
$\delta^2(k,\theta,\theta_T)$
0.3251 x 10^{-3}
0.2471 x 10^{-3}
0.108 x 10^{-3}
θ = 0
θ = 21
θ = 39
θ = 60
θ = 21
θ = 0
0 5 10 20 30 40 50 60 70 75
K
B

Fig.III.10

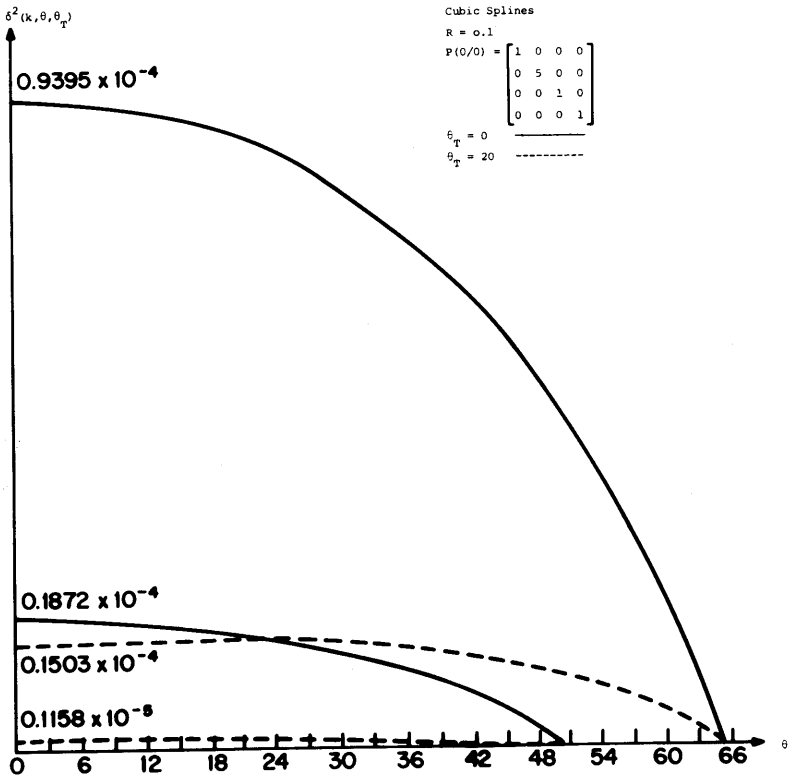
$\delta^2(k,\theta,\theta_T)$
Cubic Splines
R = o.1
P(0/0) = [1 0 0 0; 0 5 0 0; 0 0 1 0; 0 0 0 1]
θ_T = 0
θ_T = 20
0.9395 x 10^{-4}
0.1872 x 10^{-4}
0.1503 x 10^{-4}
0.1158 x 10^{-5}
0 6 12 18 24 30 36 42 48 54 60 66
θ

A

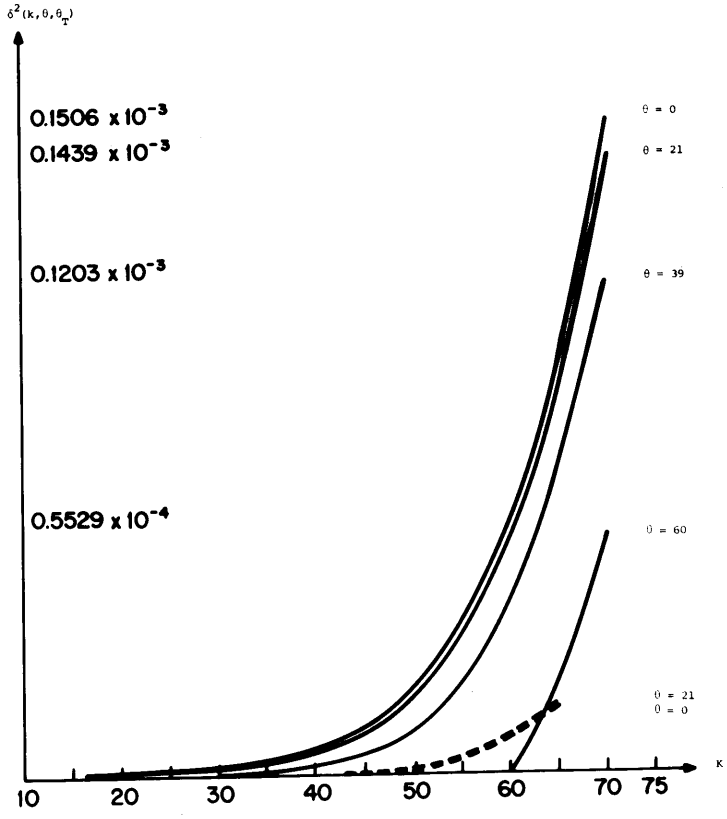
$\delta^2(k,\theta,\theta_T)$
0.1506 x 10^{-3}
0.1439 x 10^{-3}
0.1203 x 10^{-3}
0.5529 x 10^{-4}
θ = 0
θ = 21
θ = 39
θ = 60
θ = 21
θ = 0
10 20 30 40 50 60 70 75
K

B

Fig.III.11

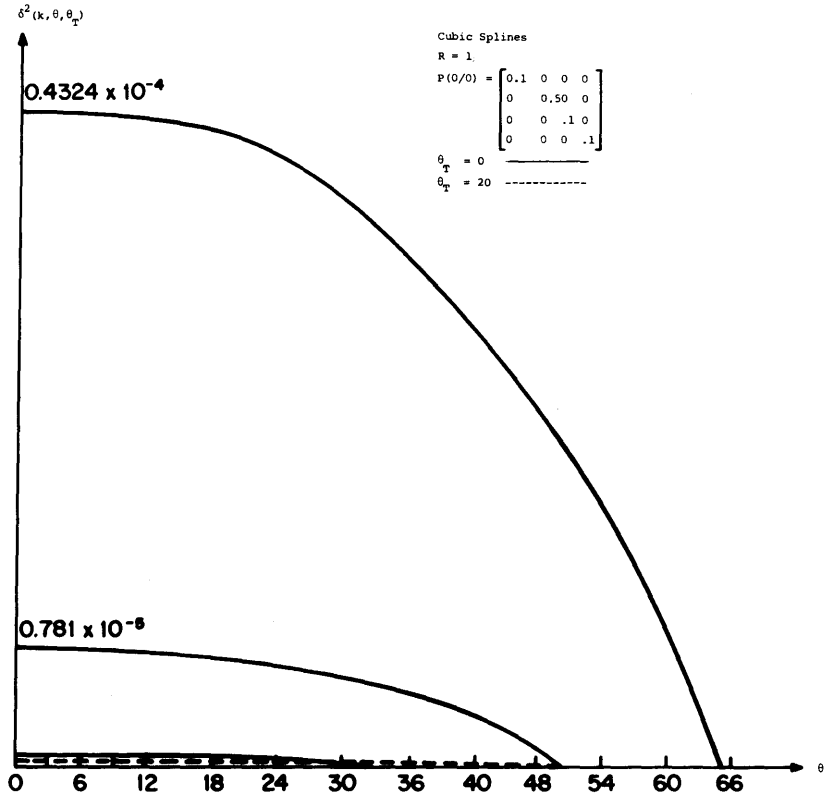
$\delta^2(k,\theta,\theta_T)$
Cubic Splines
R = 1
P(0/0) = [0.1 0 0 0; 0 0.50 0 0; 0 0 .1 0; 0 0 0 .1]
θ_T = 0
θ_T = 20
0.4324 x 10⁻⁴
0.781 x 10⁻⁵
0 6 12 18 24 30 36 40 48 54 60 66
θ

A

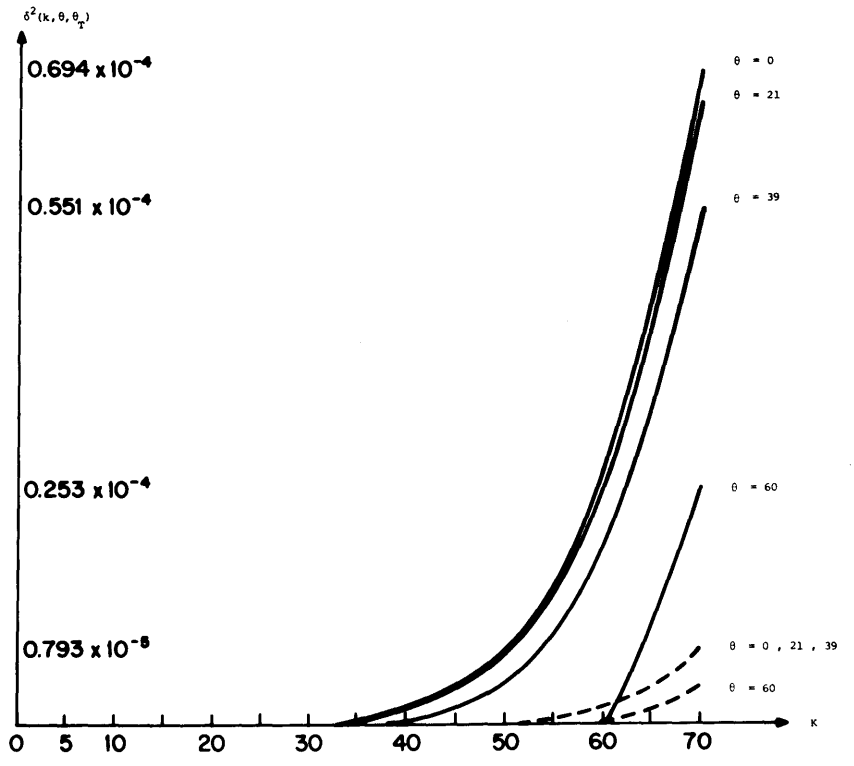
$\delta^2(k,\theta,\theta_T)$
0.694 x 10⁻⁴
0.551 x 10⁻⁴
0.253 x 10⁻⁴
0.793 x 10⁻⁵
θ = 0
θ = 21
θ = 39
θ = 60
θ = 0 , 21 , 39
θ = 60
0 5 10 20 30 40 50 60 70
K

B

Fig.III.12

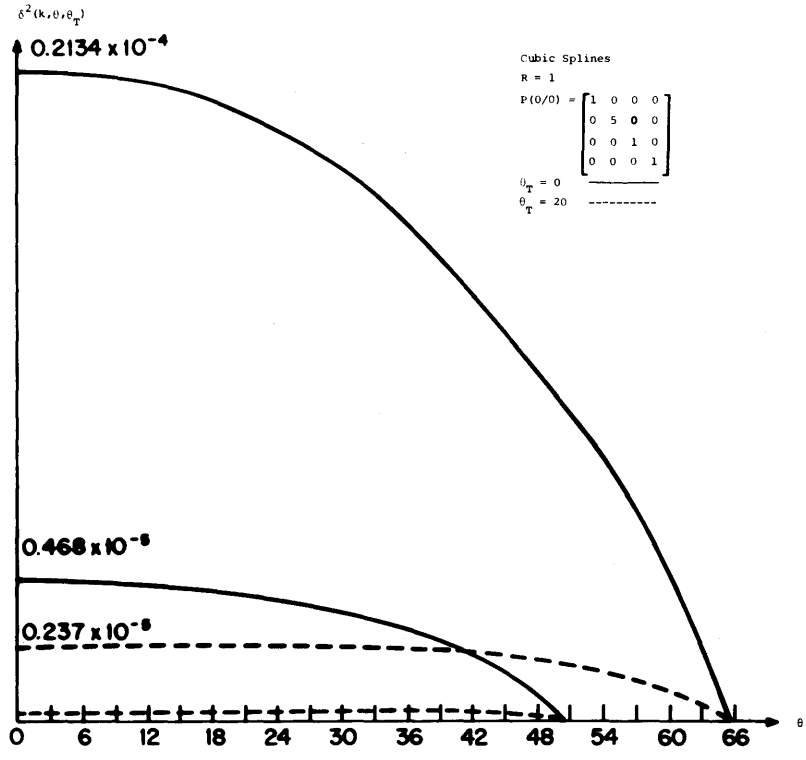
$\delta^2(k,\theta,\theta_T)$
0.2134 x 10^{-4}
Cubic Splines
R = 1
P(0/0) = [1 0 0 0; 0 5 0 0; 0 0 1 0; 0 0 0 1]
θ_T = 0
θ_T = 20
0.468 x 10^{-8}
0.237 x 10^{-8}
0 6 12 18 24 30 36 42 48 54 60 66
θ

A

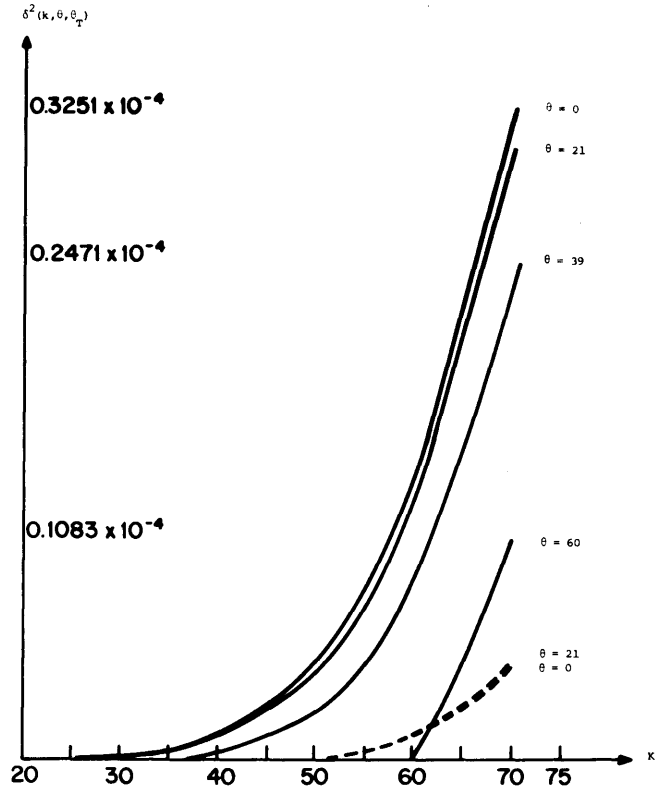
$\delta^2(k,\theta,\theta_T)$
0.3251 x 10^{-4}
0.2471 x 10^{-4}
0.1083 x 10^{-4}
θ = 0
θ = 21
θ = 39
θ = 60
θ = 21
θ = 0
20 30 40 50 60 70 75
K

B

Fig.III.13

two different ways :

1) as a function of Θ, with parameter Θ_T and several values of k, and

2) as a function of k, with parameter Θ and several values of Θ_T.

Recall that : k = actual time

Θ = time of failure as hypothesized by GLR

Θ_T = true time of the failure

There we have taken = 1 for simplicity. Several outstanding facts can be pointed out :

A) The noncentrality parameter δ^2 has its maximum value for $\Theta = \Theta_T$, for any fixed value of k.

B) The noncentrality parameter δ^2 is a nondecreasing function of k, for any fixed value of Θ_T.

C) The noncentrality parameter δ^2 has greater values for linear order splines than for any other order spline function.Here, we will be actually looking for " failures " in the first derivative.

D) Smaller values of the sensor's noise covariance R allow a much better performance of the GLR detector, increasing the size of the noncen---trality parameter δ^2. (Compare Figs. III.2a and III.4a)

E) Smaller values of P(0/0) increase the size of the noncentrality parameter δ^2 (Compare Figs. III.2a and III.3a), since the Kalman filter gain is smaller with the small P(0/0) and thus essentially the effect of the entire jump appears in the residual.

F) Smaller values of R and greater values of P(0/0) increase " knot resolution ", i.e. the noncentrality parameter δ^2 curves, as a function of θ are more peaked at θ_T when one has smaller values of R and greater values of P(0/0). (Compare Figs. III.3a and III.4a)

G) The nondecreasing δ^2 curves as a function of k approach a constant value much faster for greater values of P(0/0) for any fixed parameter θ_T. (Compare Figs. III.2b and III.3b). This most outstanding fact will allow the GLR detection scheme to be more sensitive to new information, making this approach feasible for precise multiple knot location. (This fact will be analyzed in detail in Chapter V)

H) Knot resolution increases dramatically for a decreasing order of spline function. (Compare Figs. III.10a, III.6a and III.2a) This fact ----- essentially allows us to expect a better performance of the GLR ----- approach in locating the knots of first order polynomials. Specifically , we may want to consider linear splines for ECG modeling. Of course, one would then expect to need more knots to represent the ECG.

A detailed analysis of the above tradeoffs involved in GLR design led us to choose the following guidelines for use in choosing GLR design parameters. We will analyze these issues in great detail when we discuss the -- application of the GLR technique to ECG data analysis.

1) Use as low an order for the spline approximation possible to improve

GLR performance.

2) Use of small values of the sensor noise covariance R, together with

3) Greater values of the elements of the error covariance matrix P(0/0).

III.2) Multiple Knots

Up to this point, we have dealt with failure detection systems whose --- main concern was the identification of a single failure. We intend now to develop some useful equations for the multiple failure identification problem.

Consider first the two failure problem. Define :

θ_{T1} = true time of failure # 1

θ_{T2} = true time of failure # 2

Due to the linearity of the system and filter, the residuals $\gamma(k)$ can be written as :

$$\gamma(k) = \gamma_I(k) + \gamma_{II}(k) + \gamma_{III}(k) \qquad \text{(III.2.1)}$$

where : $\gamma_I(k)$ corresponds to all effects except θ_{T1} , θ_{T2} and υ

$\gamma_{II}(k)$ corresponds to the effects of θ_1 and υ

$\gamma_{III}(k)$ corresponds to the effects of θ_2 and υ

Substituting equation III.2.1 (superposition of the effect of the residuals) into the definition of the matrix $d(k,\theta)$ yields :

$$d(k,\theta) = \sum_{j=1}^{k} G^T(j,\theta)\, V^{-1}(j)\, [\gamma_I(k) + \gamma_{II}(k) + \gamma_{III}(k)\,] \qquad \text{(III.2.2)}$$

Taking the expected value :

$$E\,[\,d(k,\theta)\,] = \sum_{j=1}^{k} G^T(j,\theta)\, V^{-1}(j)\, [\, G(j,\theta_{T1})F_n\alpha_1 + G(j,\theta_{T2})F_n\alpha_2 \qquad \text{(III.2.3)}$$

The noncentrality parameter δ^2 as a function of failures #1 and #2 can be written as :

$$\delta^2(\,k,\theta,\theta_{T1},\theta_{T2}) = [\,F_n^T\, E[d(k,\theta)]]^2 / F_n^T\, C(k,\theta)\, F_n$$

$$\delta^2(\,k,\theta,\theta_{T1},\theta_{T2}) = \delta^2(k,\theta,\theta_{T1}) + \delta^2(k,\theta,\theta_{T2}) + 2*\delta(k,\theta,\theta_{T1})*\delta(k,\theta,\theta_{T2}) \qquad \text{(III.2.4)}$$

We have computed the value of this quantity in several cases for linear splines. The actual computer program used the following values :

$n = 2$

$R = 0.1$

$$P(0/0) = \begin{bmatrix} 1.0 & 0.0 \\ 0.0 & 5.0 \end{bmatrix}$$

$\alpha_1 = \alpha_2 = 1.0$

Three different pairs of knot locations were chosen :

a) $\theta_{T1} = 20 \quad \theta_{T2} = 40$

b) $\theta_{T1} = 20 \quad \theta_{T2} = 70$

c) $\theta_{T1} = 20 \quad \theta_{T2} = 100$

The results are plotted in Fig. III.14, which shows the noncentrality parameter $\delta^2(k,\theta,\theta_{T1},\theta_{T2})$ as a function of θ, with parameter (θ_{T1},θ_{T2}) and several values of k.

It can be seen, that GLR does have difficulty in resolving the two knots. It is this observation that has led us to consider " age weighted " fil-- tering. (Chapter V)

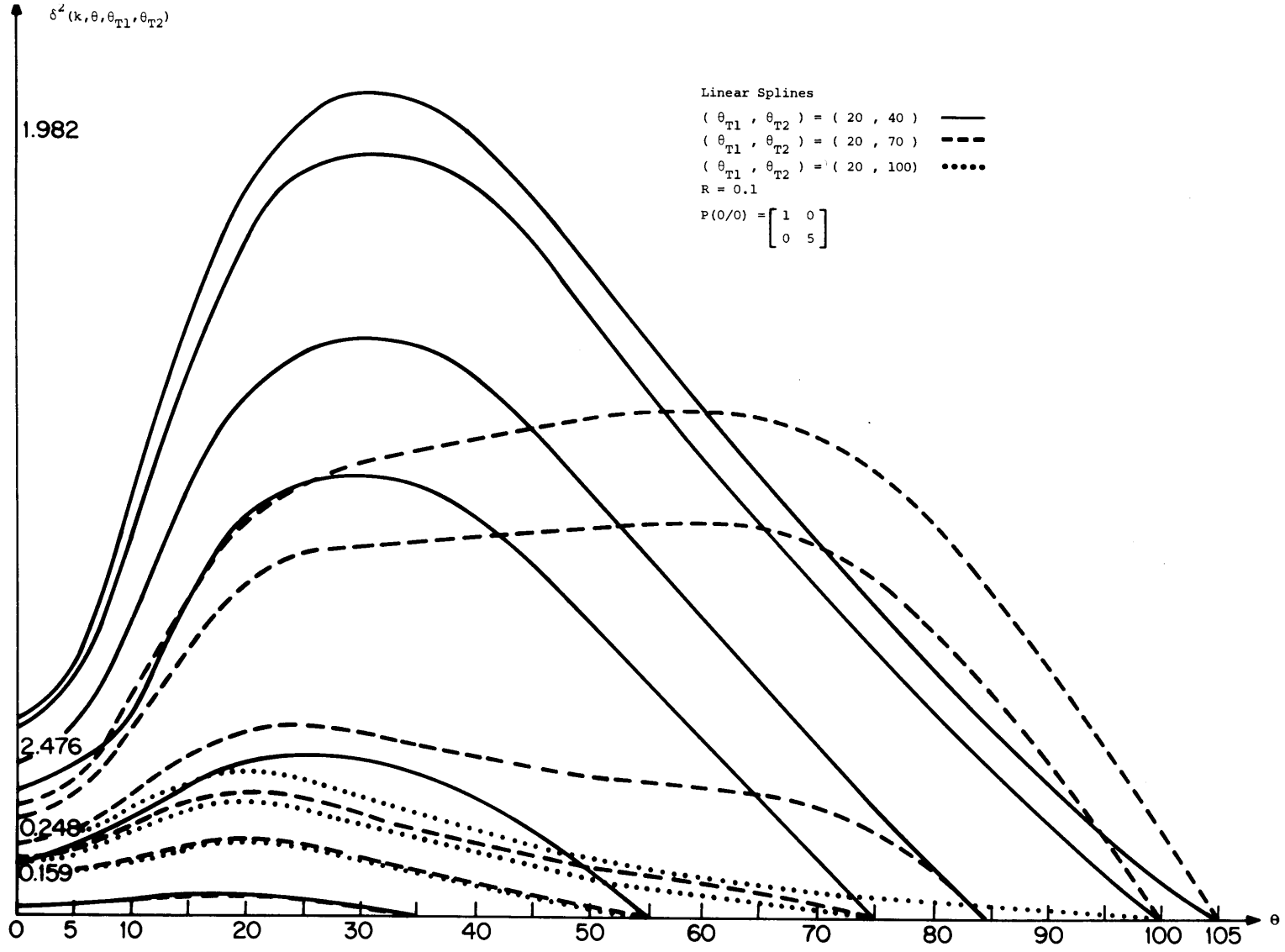
$\delta^2(k,\theta,\theta_{T1},\theta_{T2})$
1.982
2.476
0.248
0.159
Linear Splines
(θ_{T1} , θ_{T2}) = (20 , 40)
(θ_{T1} , θ_{T2}) = (20 , 70)
(θ_{T1} , θ_{T2}) = (20 , 100)
R = 0.1
P(0/0) = [1 0; 0 5]
0 5 10 20 30 40 50 60 70 80 90 100 105
θ

Fig.III.14

Chapter IV

Sensitivity Equations

IV.1) Development of the Sensitivity Equations for the Noncentrality Parameter $\delta^2(k,\theta,\theta_T)$

In the last Chapter we developed some computer programs for the computation of the noncentrality parameter δ^2. There we used arbitrary values for the parametric vector $\alpha(0)$, where $\alpha(k)$ is defined as :

$$\alpha(k) = \begin{bmatrix} R \\ P_{11}(k/k) \\ P_{12}(k/k) \\ \vdots \\ P_{nn}(k/k) \end{bmatrix} \qquad \text{(IV.1.1)}$$

The obtained results have allowed us to derive some useful properties of our knot location detector.

In our search for the tradeoffs involved in the choice of the detection system parametric vector $\alpha(0)$, we will develop the so called " sensitivity equations ". By doing this, we will be able to get precise knowledge of how system parameters affect the noncentrality parameter δ^2. As given by expression (II.3.3), δ^2 can be computed with knowledge of the information matrices $C(k,\theta)$ and $C(k,\theta,\theta_T)$, which are in fact linear functions of the failure signature matrices $G(k,\theta)$ and $G(k,\theta_T)$.

The necessary quantities for the evaluation of the failure signature --- matrices were given in section II.1 .Thus, straightforward calculations lead us to the following expression for the noncentrality parameter ---- $\delta^2(k+1,\theta,\theta_T)$:

$$\delta^2(k+1,\theta,\theta_T) = f(\ F(k-1,\theta),F(k-1,\theta_T),\ \alpha(k-1)) \qquad \text{(IV.1.2)}$$

Notice the dependence of the above expression on functions evaluated at time (k-1) .

IV.2) Taylor Series Expansion for $\delta^2(k+1,\theta,\theta_T)$

Consider incrementing the parametric vector $\alpha(k-1)$ by$\Delta\alpha(k-1)$ around its nominal value $\alpha^0(k-1)$. The expression IV.1.2 for the noncentrality parameter $\delta^2(k+1,\theta,\theta_T)$ will consequently be incremented by the value ------- $\Delta\delta^2(k+1,\theta,\theta_T)$ around its nominal value$\delta^2(k+1,\theta,\theta_T)^0$. Thus, making a --- Taylor Series expansion of the noncentrality parameter (expression IV. 1.2) around its nominals yields after simplification :

$$\Delta\delta^2(k+1,\theta,\theta_T) = \left[\frac{\partial f}{\partial F(k-1)}\right]_{NOM.} \Delta F(k-1) + \left[\frac{\partial f}{\partial \alpha(k-1)}\right]_{NOM.} \Delta\alpha(k-1)$$

$$+ \text{h.o.t.} \qquad \text{(IV.2.1)}$$

where : $F(k-1) = \begin{bmatrix} F_{11}(k-1,\theta) \\ F_{12}(k-1,\theta) \\ \vdots \\ F_{nn}(k-1,\theta) \\ F_{11}(k-1,\theta_T) \\ F_{12}(k-1,\theta_T) \\ \vdots \\ F_{nn}(k-1,\theta_T) \end{bmatrix}$ (IV.2.2)

In expression (IV.2.1), h.o.t. refers to quadratic, cubic, quartic, ... etc. terms of the Taylor Series. The key property of the h.o.t. is that :

$$\lim_{\Delta\delta^2(k+1,\theta,\theta_T)\to 0} \frac{\| \text{h.o.t.} \|}{\| \Delta\delta^2(k+1,\theta,\theta_T) \|} = 0$$

If we examine (IV,2.1) and assume that $\Delta\delta^2(k+1,\theta,\theta_T)$ is very small, we can approximate the exact expression (IV.2.1) by :

$$\frac{\Delta\delta^2(k+1,\theta,\theta_T)}{\Delta\alpha} = \left.\frac{\partial f}{\partial F(k-1)}\right]_{NOM.} \Delta F(k-1) + \left.\frac{\partial f}{\partial \alpha(k-1)}\right]_{NOM.} \Delta\alpha(k-1) \quad \text{(IV.2.3)}$$

Dividing the above equation by $\Delta\alpha_i(k-1)$ we get the sensitivity equation for the noncentrality parameter δ^2, namely :

$$\frac{\Delta\delta^2(k+1,\theta,\theta_T)}{\Delta\alpha_i(k-1)} = \left[\frac{\partial f}{\partial F(k-1)}\right]_{NOM.} \frac{\Delta F(k-1)}{\Delta\alpha_i(k-1)} + \left[\frac{\partial f}{\partial \alpha_i(k-1)}\right]_{NOM.} \qquad \text{(IV.2.4)}$$

In this research we did not make use of this analysis to determine " --- good " values for the design parameters $\alpha(0)$. For completeness, we pre-- sent a detailed derivation of the required equations leading to the evaluation of the sensitivity expression for the noncentrality parameter δ^2. using linear splines.

For this particular case, the parametric vector $\alpha(k-1)$ and the vector $F(k-1)$ take the following form :

$$\alpha(k-1) = \begin{bmatrix} R \\ P_{11}(k-1/k-1) \\ P_{12}(k-1/k-1) \\ P_{22}(k-1/k-1) \end{bmatrix} \quad , \quad F(k-1) = \begin{bmatrix} F_{11}(k-1,\theta) \\ F_{12}(k-1,\theta) \\ F_{21}(k-1,\theta) \\ F_{22}(k-1,\theta) \\ F_{11}(k-1,\theta_T) \\ F_{12}(k-1,\theta_T) \\ F_{21}(k-1,\theta_T) \\ F_{22}(k-1,\theta_T) \end{bmatrix} \qquad \text{(IV.2.5)}$$

Substitution of the defining expressions for the information matrices

$C(k,\theta)$ and $C(k,\theta,\theta_T)$, [Chapter II.1] into the equation for the noncentrality parameter δ^2 (II.3.3) evaluated at time (k+1) yields :

$$\delta^2(k+1,\theta,\theta_T) = \frac{\left[\sum_{j=Max(\theta,\theta_T)}^{k+1} b(j,\theta)\, b(j,\theta_T)/\, \beta(j+1)\right]^2}{\left[\sum_{j=0}^{k+1} b(j,\theta)^2/\, \beta(j+1)\right]} \qquad \text{(IV.2.6)}$$

where :

$$\beta(j+1) = H\, e^{A\Delta}\, P(j+1/j+1)\, (e^{A\Delta})^T\, H^T + R \qquad \text{(IV.2.7)}$$

$$b(j,\theta)\, b(j,\theta_T) = F_n^T\, G(j+1,\theta)^T\, G(j+1,\theta_T)\, F_n \qquad \text{(IV.2.8)}$$

After some straghtforward calculations, the above defining equations for $\beta(j+1)$ and $b(j,\theta)\, b(j,\theta_T)$ can be explicitly written as a function of the parametric vector $\alpha(k-1)$ and the vector $F(k-1)$ in the following form :

$$b(j,\theta) = \Delta^{j-\theta} + \Delta - F_{12}(j-1,\theta) - 2\Delta\, F_{22}(j-1,\theta) - (K_{11}(j) + \Delta\, K_{21}(j))(\Delta^{j-\theta} - F_{12}(j-1,\theta) - \Delta\, F_{22}(j-1,\theta)) \qquad \text{(IV.2.9)}$$

$$\beta(j+1) = \frac{[\ (\ 2P_{11}(j/j) + 6\Delta\, P_{12}(j/j) + 5\Delta^2\, P_{22}(j/j) + R\ )R + \Delta^2\, P_{11}\, P_{22}(j/j)\ ]}{b(j)} \qquad \text{(IV.2.10)}$$

where :

$$b(j) = P_{11}(j/j) + 2\Delta\, P_{12}(j/j) + \Delta^2\, P_{22}(j/j) + R \qquad \text{(IV.2.11)}$$

$$P_{11}(j/j) = \frac{R\,(\,P_{11}(j\text{-}1/j\text{-}1) + 2\Delta\, P_{12}(j\text{-}1/j\text{-}1) + \Delta^2\, P_{22}(j\text{-}1/j\text{-}1))}{\beta(j\text{-}1)} \qquad \text{(IV.2.12)}$$

$$P_{12}(j/j) = \frac{R\,(\,P_{12}(j\text{-}1/j\text{-}1) + \Delta\, P_{12}(j\text{-}1/j\text{-}1))}{\beta(j\text{-}1)} \qquad \text{(IV.2.13)}$$

$$P_{22}(j/j) = \frac{P_{22}(j\text{-}1/j\text{-}1)\;(\,P_{11}(j\text{-}1/j\text{-}1) + R\,) - P_{12}(j\text{-}1/j\text{-}1)^2}{\beta(j\text{-}1)} \qquad \text{(IV.2.14)}$$

$$K_{11}(j) = P_{11}(j\text{-}1/j\text{-}1) \;/\; R \qquad \text{(IV.2.15)}$$

$$K_{21}(j) = P_{12}(j\text{-}1/j\text{-}1) \;/\; R \qquad \text{(IV.2.16)}$$

Finally, using expressions (IV.2.9) through (IV.2.16) and differentiating (IV.2.6) with respect to some of the elements of the parametric vector $\alpha(k\text{-}1)$ yields the corresponding sensitivity equation. Differentiation is straightforward, but the resulting expressions sre rather complicated and will be omitted here.

Chapter V

Age Weighting Filtering

V.1) The Single Knot Case

As noted in Chapter II, the GLR detection scheme uses a discrete Kalman filter based on a " no jump " assumption for information processing. It is clear, that the filter bases its estimate on all the available information. Assume, however, that the dynamics for our heart model are imprecisely --- known. Then, the Kalman filter might " learn " the state " too well ". Because of imprecise dynamics used in the filter, the " good " estimate may be wrong. In the literature this is referred to as the problem of ---- filter divergence. [7]

A reasonable approach to this problem is to limit the filter memory so that the estimate does not become too " good ". By limiting the filter memory we mean computing an estimate conditioned on data from only the " recent past ". This has the effect of preventing the error covariance matrix P(k/k) from becoming too small, hence preventing the Kalman filter gain from becoming very small. Discarding old data can be accomplished by ----- weighting them according to when they occurred, as shown in Fig. V.1. This means that the sensor noise covariance R must somehow be " increased " for past measurements, as illustrated in Fig. V.2.

Assume exponential age weghting of old data :

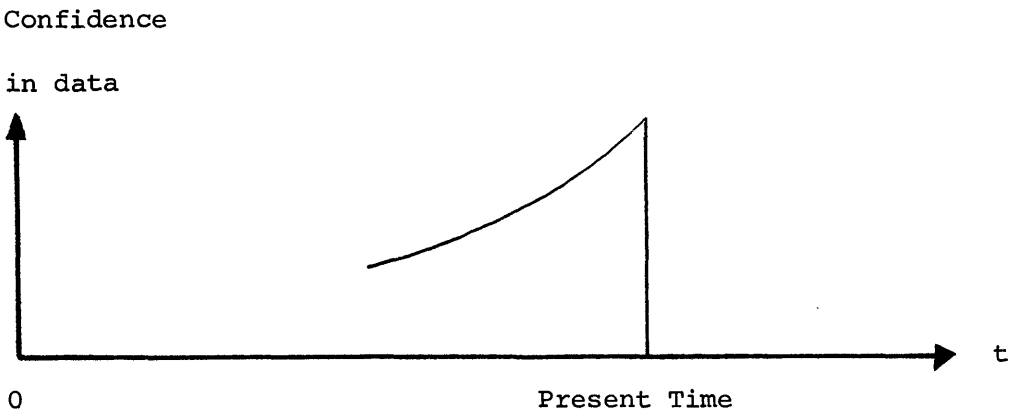

Fig.V.1

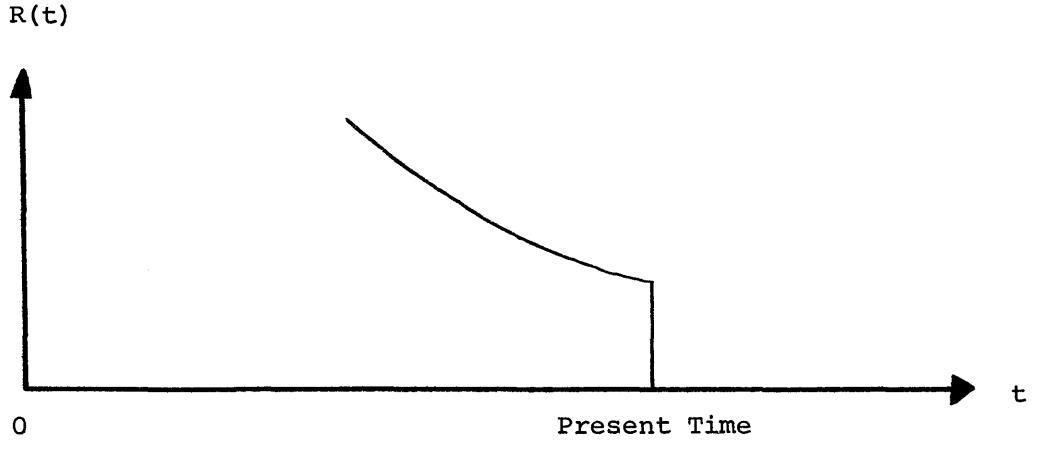

Fig.V.2

$$R(k-1) = e^{1/x} R(k) \qquad (V.1.1)$$

for $k > 1$ and $x > 0$

where : x is the age weighting time constant.

A recursive Kalman filter can be constructed under these assumptions [7]

The equations are :

Error covariance update :

$$P(k-1/k-1) = e^{1/x} [I - K(k-1) H] P(k-1/k-2) \qquad (V.1.2)$$

Error covariance extrapolation :

$$P(k/k-1) = e^{A\Delta} P(k-1/k-1) (e^{A\Delta})^T \qquad (V.1.3)$$

Residual covariance :

$$V(k) = H P(k/k-1) H^T + e^{-1/x} R \qquad (V.1.4)$$

Kalman filter gain :

$$K(k) = P(k/k-1) H^T V^{-1}(k) \qquad (V.1.5)$$

A computer program for computing the noncentrality parameter $\delta^2(k,\theta,\theta_T)$ incorporating the age-weghted filtering concept was written and tested for the following age-weghting time constants :

a) x = 10

b) x = 50

The analysis tests were run for the linear spline case using the following

set of parameters :

$$R = 0.1 \quad , \quad P(0/0) = \begin{bmatrix} 1.0 & 0.0 \\ 0.0 & 5.0 \end{bmatrix}$$

Results are presented in Figs. V.3 through V.5. Fig V.3 (age-weighting constant x = 10) and Fig. V.4 (age-weighting constant x = 50) show the noncentrality parameter δ^2 as a function of k, with parameter θ for two different values of θ_T. In Fig. V.5, the noncentrality parameter δ^2 has been plotted as a function of θ, with parameter θ_T, for k = 25 and k = 50. For comparison we have plotted both noncentral δ^2 curves (x = 10 and --- x = 50) on the same Fig. V.5 .

Two facts can be pointed out :

A) The noncentrality parameter $\delta^2(k,\theta,\theta_T)$ curves as a function of k (Fig. V.3 and V.4) reach a final constant value much faster as we increase the noise covariance R exponentially for past measurements, i.e. as we reduce the exponential age-weighting time constant x . This fact essentially allows the GLR detector to be more sensitive to new information (basically discarding its past history).

B) It can be seen (Fig. V.5) , that the noncentrality parameter $\delta^2(k,\theta,\theta_T)$ curves are less peaked as a function of θ as we add more age-weighting. This is a direct consequence of the exponentially increased noise covariance R, which actually supports our initial comments in Chapter III.1.

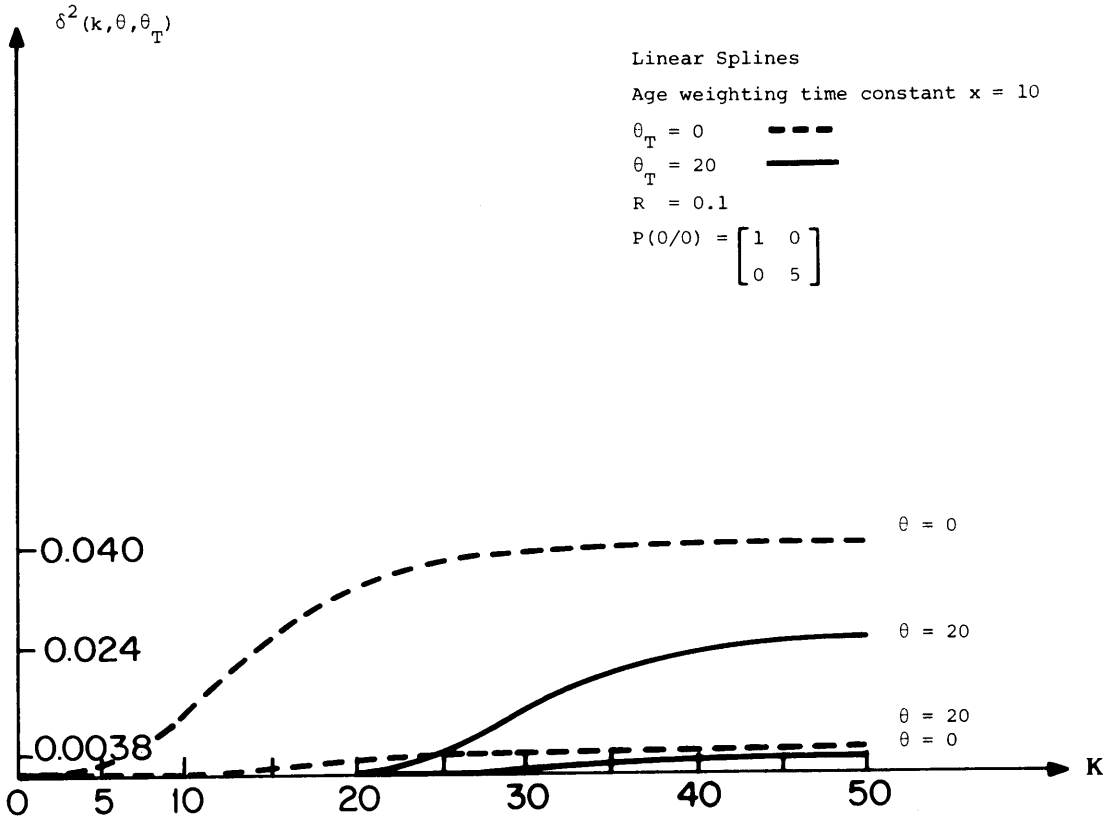
$\delta^2(k,\theta,\theta_T)$
Linear Splines
Age weighting time constant x = 10
θ_T = 0
θ_T = 20
R = 0.1
P(0/0) = [1 0; 0 5]
θ = 0
θ = 20
θ = 20
θ = 0
0.040
0.024
0.0038
0
5
10
20
30
40
50
K

Fig.V.3

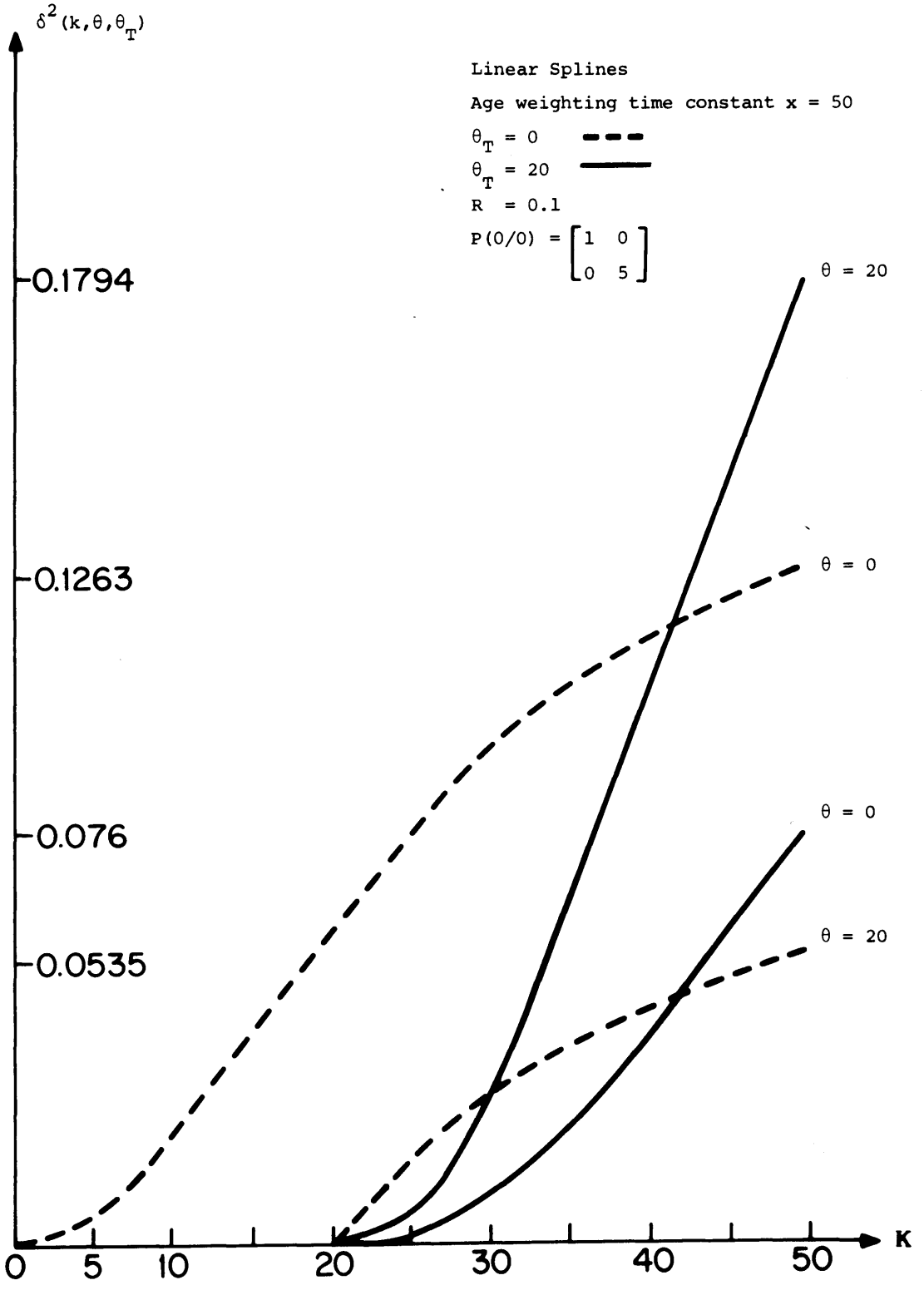
$\delta^2(k,\theta,\theta_T)$
Linear Splines
Age weighting time constant x = 50
θ_T = 0
θ_T = 20
R = 0.1
P(0/0) = [1 0; 0 5]
0.1794
0.1263
0.076
0.0535
θ = 20
θ = 0
θ = 0
θ = 20
0
5
10
20
30
40
50
K

Fig.V.4

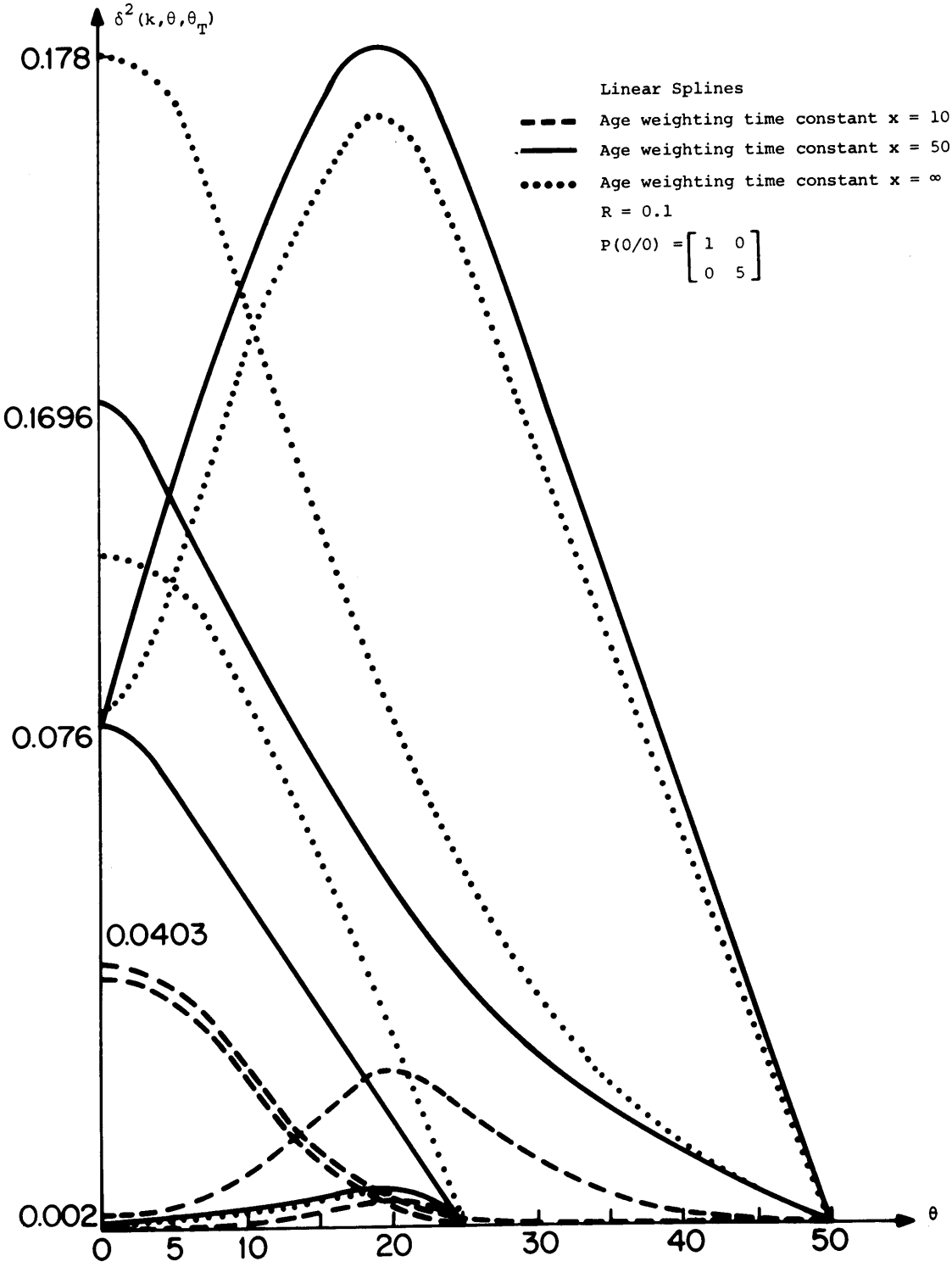
$\delta^2(k,\theta,\theta_T)$
0.178
0.1696
0.076
0.0403
0.002
0
5
10
20
30
40
50
θ
Linear Splines
Age weighting time constant x = 10
Age weighting time constant x = 50
Age weighting time constant x = ∞
R = 0.1
P(0/0) = [1 0; 0 5]

Fig.V.5

V.2) Age Weighted Multiple Knot Location

As mentioned in Chapter III, the GLR detector has difficulty in resolving the two knot location problem. Limiting the filter memory to data from -- only the recent " past " seems now to be a reasonable approach to over--- come this trouble.

The exponential age-weighting filtering concept was analyzed for the two knot location problem. A Fortran computer program incorporating this --- filtering concept was developed and tested for two different pairs of --- knot locations :

a) $\theta_{T1} = 20 \qquad \theta_{T2} = 40$

b) $\theta_{T2} = 20 \qquad \theta_{T2} = 70$

Results are plotted in Fig. V.6 (age-weighting time constant x = 10) and Fig. V.7 (age-weighting time constant x = 50), where the noncentrality parameter $\delta^2(k,\theta,\theta_{T1},\theta_{T2})$ is shown as a function of θ, for the selected sets of parameters a) and b) and several values of k.

Some important facts can be mentioned :

A) The size of the noncentrality parameter $\delta^2(k,\theta,\theta_{T1},\theta_{T2})$ decreases as we decrease the age-weighting time constant x for some fixed value of k. (Compare Fig. V.6 and Fig. V.7)

B) As we add more age-weighting, i.e. as we decrease the age-weighting time constant x, the knot resolution for the noncentrality parameter -------

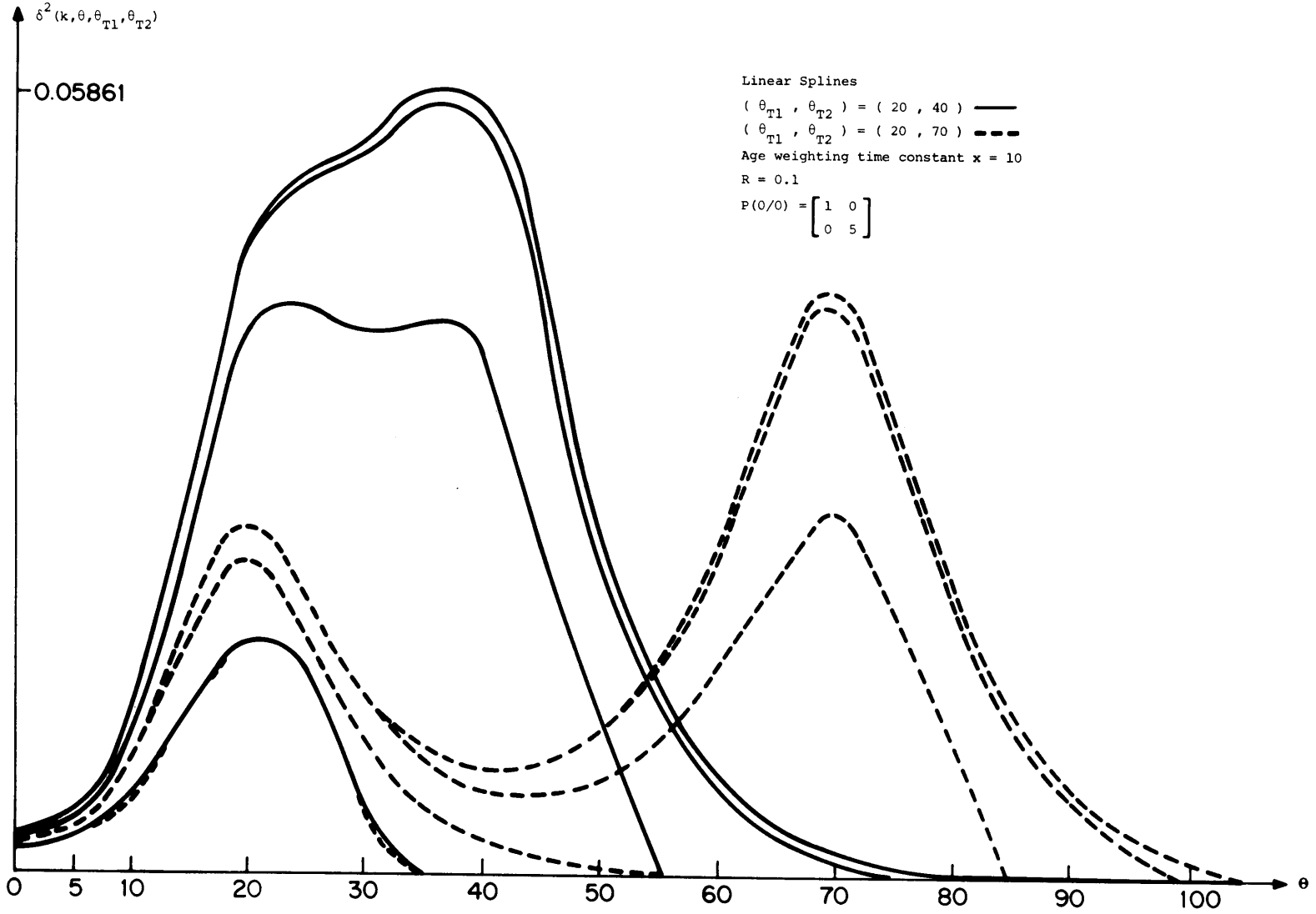
$\delta^2(k,\theta,\theta_{T1},\theta_{T2})$
0.05861
Linear Splines
(θ_{T1} , θ_{T2}) = (20 , 40)
(θ_{T1} , θ_{T2}) = (20 , 70)
Age weighting time constant x = 10
R = 0.1
P(0/0) = [1 0; 0 5]
0 5 10 20 30 40 50 60 70 80 90 100
θ

Fig.V.6

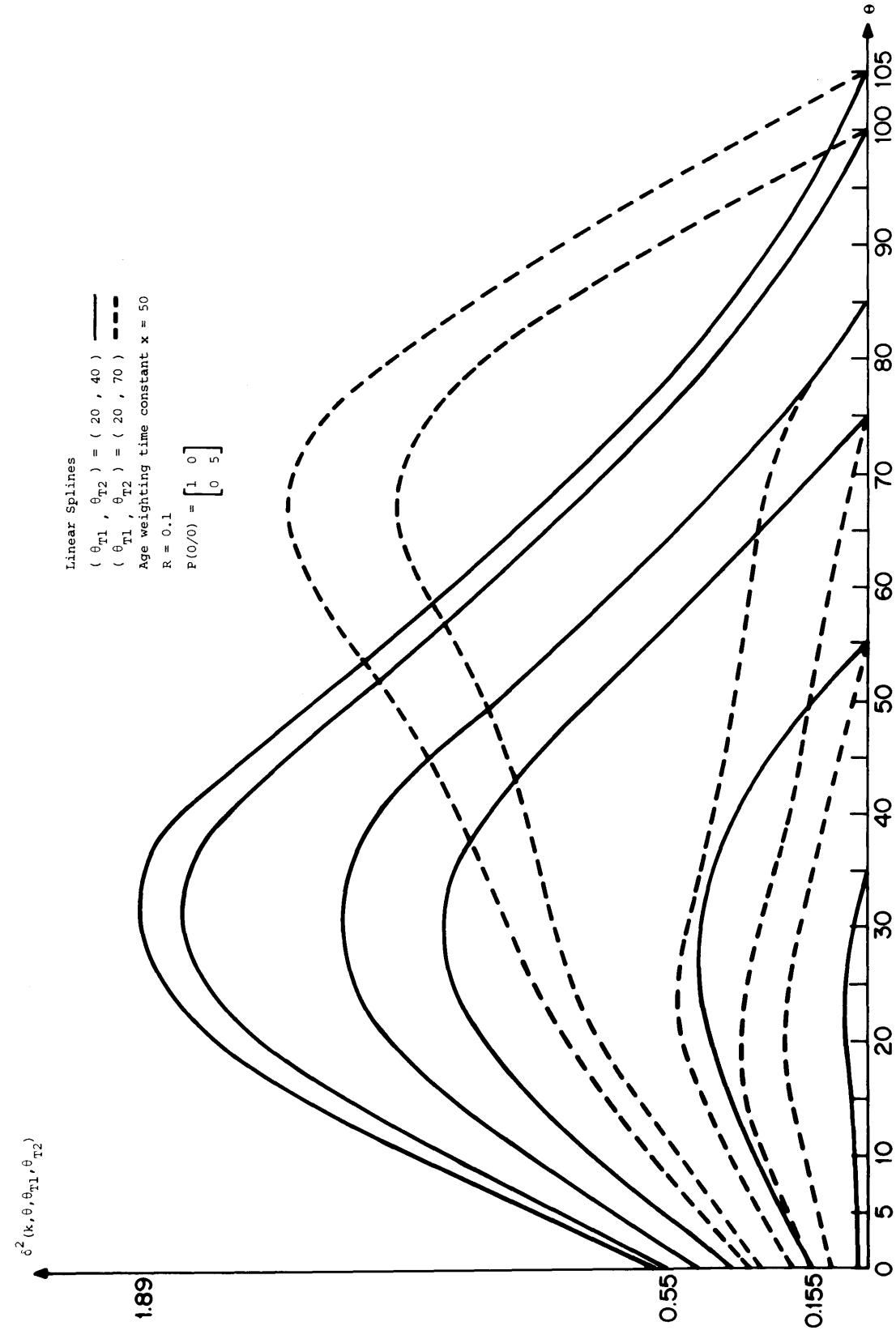
Linear Splines
(θT1 , θT2) = (20 , 40)
(θT1 , θT2) = (20 , 70)
Age weighting time constant x = 50
R = 0.1
P(0/0) = [1 0; 0 5]
δ²(k,θ,θT1,θT2)
1.89
0.55
0.155
0
5
10
20
30
40
50
60
70
80
90
100
105
θ

Fig.V.7

$\delta^2(k,\theta,\theta_{T1},\theta_{T2})$ curves increases considerably (Fig. V.6)

C) Knot resolution increases as the knots to be located are more separa-- ted from each other (See Fig. V.6)

V.3) Discussion

The inclusion of the age-weighting concept as part of the Kalman filter used for information processing has given us a new input variable that we can use to adjust GLR detector performance.

As mentioned earlier in this work, our basic objective will be to determine the feasibility of using spline functions for ECG modeling. The --- approximation problem requires that the adaptive knot location of a mesh of knots :

$$\theta : \quad \theta_{T1} < \theta_{T2} < \quad \ldots \quad < \theta_{TN}$$

which will divide ECG data into N different subregions. Thus, although -- for single knot detection purposes we might want to use larger values for the age-weighting time constant x, i.e. we may want large values of the noncentrality parameter $\delta^2(k,\theta,\theta_T)$, the adaptive knot location of the -- mesh of knots θ demands fine knot resolution, available only when we use small values for the age-weighting time constant.

Moreover, since knot resolution is poor when, in fact, the knots to be located are close to each other, we will consider a " dead-zone " time interval for identification purposes, i.e. we will avoid knot location for some time after a knot θ_{T_i} has been located.

Chapter VI

Experimental Research

VI.1) Knot Location for ECG Approximation

The analytical work developed thus far in this research has provided us with some understanding of GLR performance in locating knots when we actually observe a spline in additive Gaussian noise. Now we plan to determine the feasibility of using such an approach when we wish to approximate waveforms that are not splines, i.e. specifically ECG's. In Fig. VI.1 we have shown a typical heartbeat cycle as recorded on an electrocardiogram. We note that the ECG consists of a sequence of waves (P, Q, R, S and T), and, if it is to be successful, the GLR detector should determine their location. In addition, given the high amplitude and frequency content of the QRS complex [10], we would expect a higher " knot density " in this region .

A Fortran computer program for the CGLR detection scheme was developed and used to process ECG data. The data was digitized ECG data, sampled at 250 Hz (time interval Δ = 4 msec.) . In addition to the CGLR system as discussed so far, we have included a feedback path for incrementing the Kalman filter estimate and covariance subsequent to the detection of a -- knot (see [6]). A flow chart for our program is presented in Fig. VI.2.

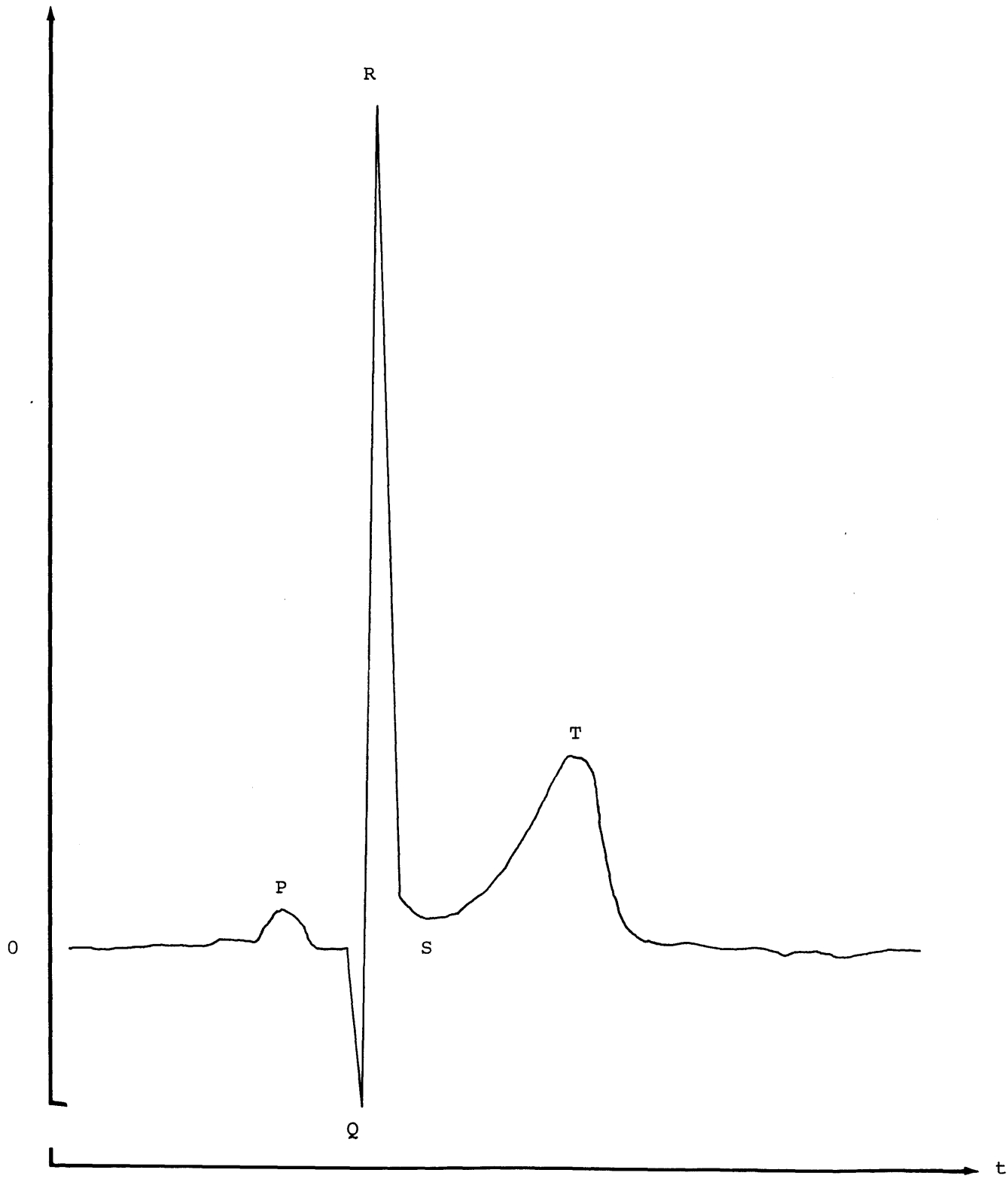

Fig. VI.1

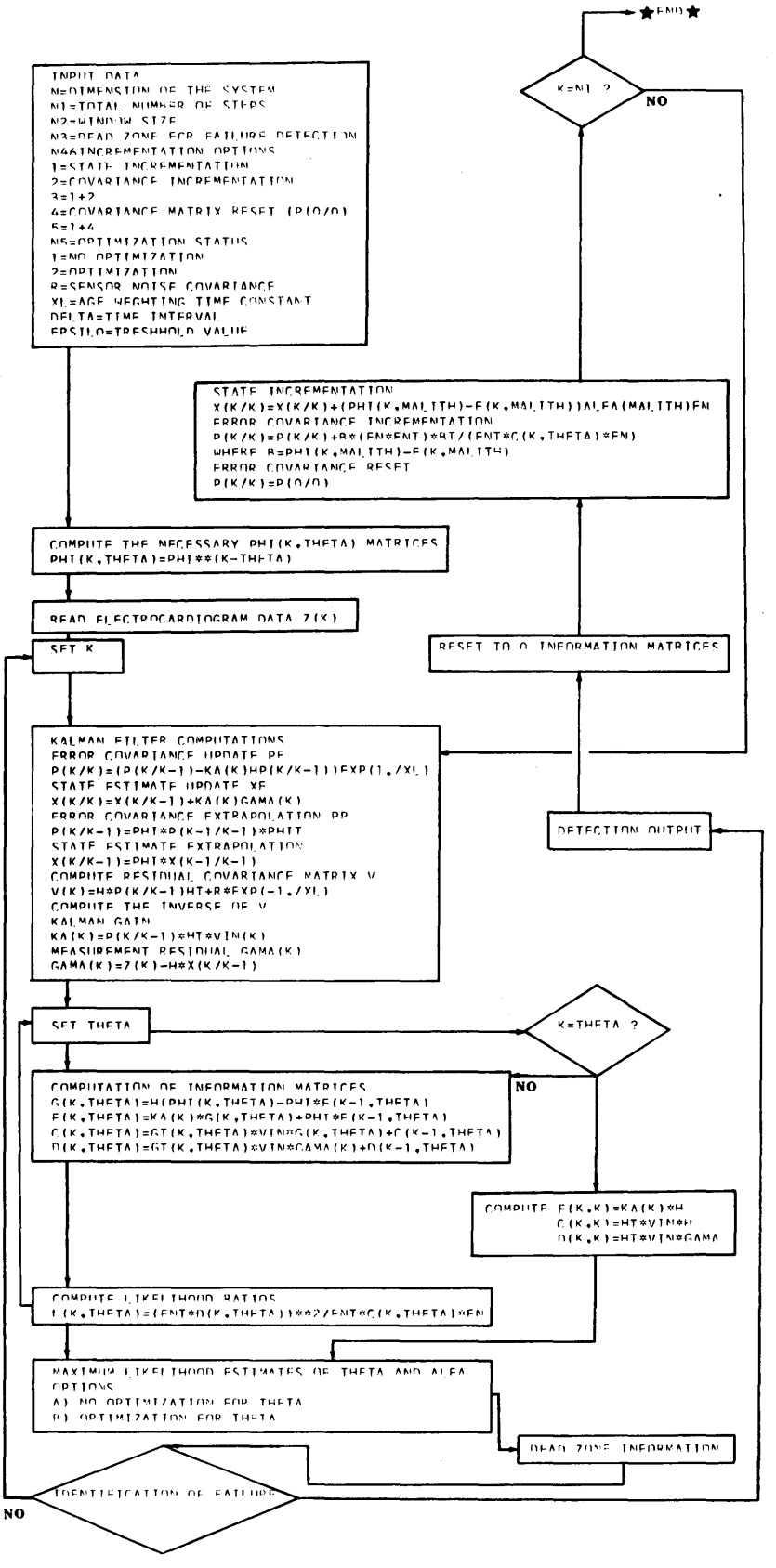
INPUT DATA
N=DIMENSION OF THE SYSTEM
N1=TOTAL NUMBER OF STEPS
N2=WINDOW SIZE
N3=DEAD ZONE FOR FAILURE DETECTION
N4=INCREMENTATION OPTIONS
1=STATE INCREMENTATION
2=COVARIANCE INCREMENTATION
3=1+2
4=COVARIANCE MATRIX RESET (P(0/0)
5=1+4
N5=OPTIMIZATION STATUS
1=NO OPTIMIZATION
2=OPTIMIZATION
R=SENSOR NOISE COVARIANCE
XL=AGE WEIGHTING TIME CONSTANT
DELTA=TIME INTERVAL
EPSILO=TRESHHOLD VALUE
★END★
K=N1 ?
NO
STATE INCREMENTATION
X(K/K)=X(K/K)+(PHI(K,MALITH)-F(K,MALITH))ALFA(MALITH)EN
ERROR COVARIANCE INCREMENTATION
P(K/K)=P(K/K)+R*(EN*ENT)*RT/(ENT*C(K,THETA)*EN)
WHERE R=PHI(K,MALITH)-F(K,MALITH)
ERROR COVARIANCE RESET
P(K/K)=P(0/0)
COMPUTE THE NECESSARY PHI(K,THETA) MATRICES
PHI(K,THETA)=PHI**(K-THETA)
READ ELECTROCARDIOGRAM DATA Z(K)
SET K
RESET TO 0 INFORMATION MATRICES
KALMAN FILTER COMPUTATIONS
ERROR COVARIANCE UPDATE PF
P(K/K)=(P(K/K-1)-KA(K)HP(K/K-1))EXP(1./XL)
STATE ESTIMATE UPDATE XF
X(K/K)=X(K/K-1)+KA(K)GAMA(K)
ERROR COVARIANCE EXTRAPOLATION PP
P(K/K-1)=PHI*P(K-1/K-1)*PHIT
STATE ESTIMATE EXTRAPOLATION
X(K/K-1)=PHI*X(K-1/K-1)
COMPUTE RESIDUAL COVARIANCE MATRIX V
V(K)=H*P(K/K-1)HT+R*EXP(-1./XL)
COMPUTE THE INVERSE OF V
KALMAN GAIN
KA(K)=P(K/K-1)*HT*VIN(K)
MEASUREMENT RESIDUAL GAMA(K)
GAMA(K)=Z(K)-H*X(K/K-1)
DETECTION OUTPUT
SET THETA
K=THETA ?
NO
COMPUTATION OF INFORMATION MATRICES
G(K,THETA)=H(PHI(K,THETA)-PHI*F(K-1,THETA)
F(K,THETA)=KA(K)*G(K,THETA)+PHI*F(K-1,THETA)
C(K,THETA)=GT(K,THETA)*VIN*G(K,THETA)+C(K-1,THETA)
D(K,THETA)=GT(K,THETA)*VIN*GAMA(K)+D(K-1,THETA)
COMPUTE F(K,K)=KA(K)*H
C(K,K)=HT*VIN*H
D(K,K)=HT*VIN*GAMA
COMPUTE LIKELIHOOD RATIOS
L(K,THETA)=(ENT*D(K,THETA))**2/ENT*C(K,THETA)*EN
MAXIMUM LIKELIHOOD ESTIMATES OF THETA AND ALFA
OPTIONS
A) NO OPTIMIZATION FOR THETA
B) OPTIMIZATION FOR THETA
DEAD ZONE INFORMATION
IDENTIFICATION OF FAILURE
NO

Fig.VI.2

The following set of input parameters was chosen to remain fixed throughout these tests :

a) n = 2, i.e. linear splines for ECG modeling ,

b) x = 10, i.e. we use a small age weighting time constant to permit fine knot resolution ,

c) N4 = 5, i.e. use direct state incrementation together with error covariance reset for adaptive filtering after a knot has been located,

d) N3 = 10, i.e. we will avoid locating knots for 10x4 msec. after has -- actually been located ,

e) N2 = 10, i.e. we restrict our optimization over θ to an interval of - the form $k - 10 < \theta < k$ (we note that the $l(k,k)$ is undefined).

Initially, the analysis tests were run using ECG data corresponding to the first Lead [10] of the digitized vectocardiogram (VCG) of a normal -- patient with an average heartbeat rate of 50 heartbeats/min. Several sets of values for the noise covariance R and the elements of the error cova-- riance matrix P(0/0) were chosen. The CGLR system was implemented with -- the detection law :

$$l(k,\theta) \underset{H_0}{\overset{H_1}{\gtrless}} 3500 \qquad \text{(VI.1.1)}$$

Identification of the knots was performed in two different ways :

1) Optimizing the detection law over the data " window " of width N2 = 10, and

2) Avoiding optimization, setting : $\hat{\theta} = k - N2 + 1 = k - 9$

Results are plotted in Figs. VI.3 through VI.7 showing the location of -- the knots for the first heartbeat cycle.

Several facts can be mentioned :

A) The CGLR detection scheme using optimization over the " data window ": $k - N2 < \theta < k$ allows us to determine cardiac events more accurately. For example, -- the knot location in Fig. VI.3a (optimization) defines the P wave completely, while Fig. VI.3b (no optimization) provides misleading information concerning the duration of the P wave.

B) Smaller values for the elements of the error covariance matrix P(0/0) increase the number of knots detected for any fixed values of the --- noise covariance R and the treshhold ε . (Compare Fig. VI.4 and ----- Fig. VI.7). Since the Kalman gain is smaller with the smaller P(0/0) (see IV.2.15 and IV.2.16) , the effect of the entire jump appears essentially in the residual $\gamma(k)$, allowing the likelihood ratios ---- $l(k,\theta)$ to increase.

C) Using optimization over the " data window " and greater values of the sensor noise covariance R reduces the number of knots detected for -- any fixed values of P(0/0) and the treshhold ε (Compare Figs. VI.5a, VI.6a and VI.7a)

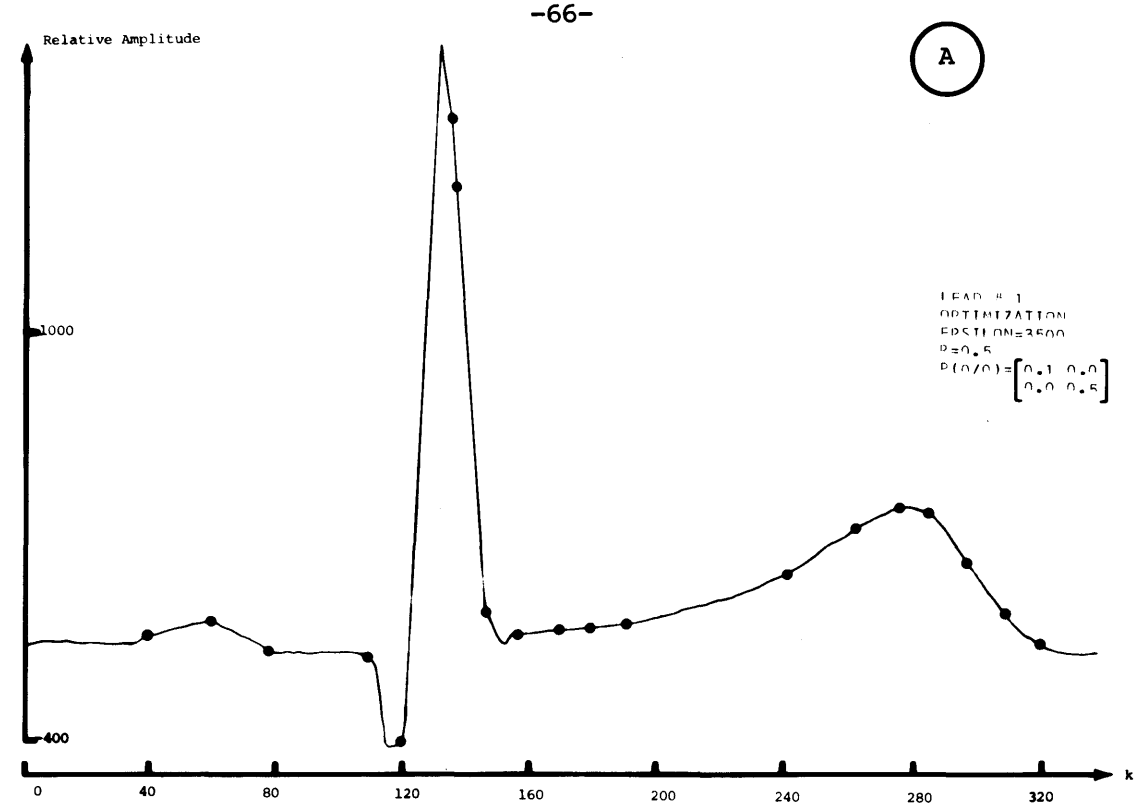
A
Relative Amplitude
1000
400
LEAD # 1
OPTIMIZATION
EPSILON=3500
P=0.5
P(0/0)=[0.1 0.0
0.0 0.5]
0
40
80
120
160
200
240
280
320
k

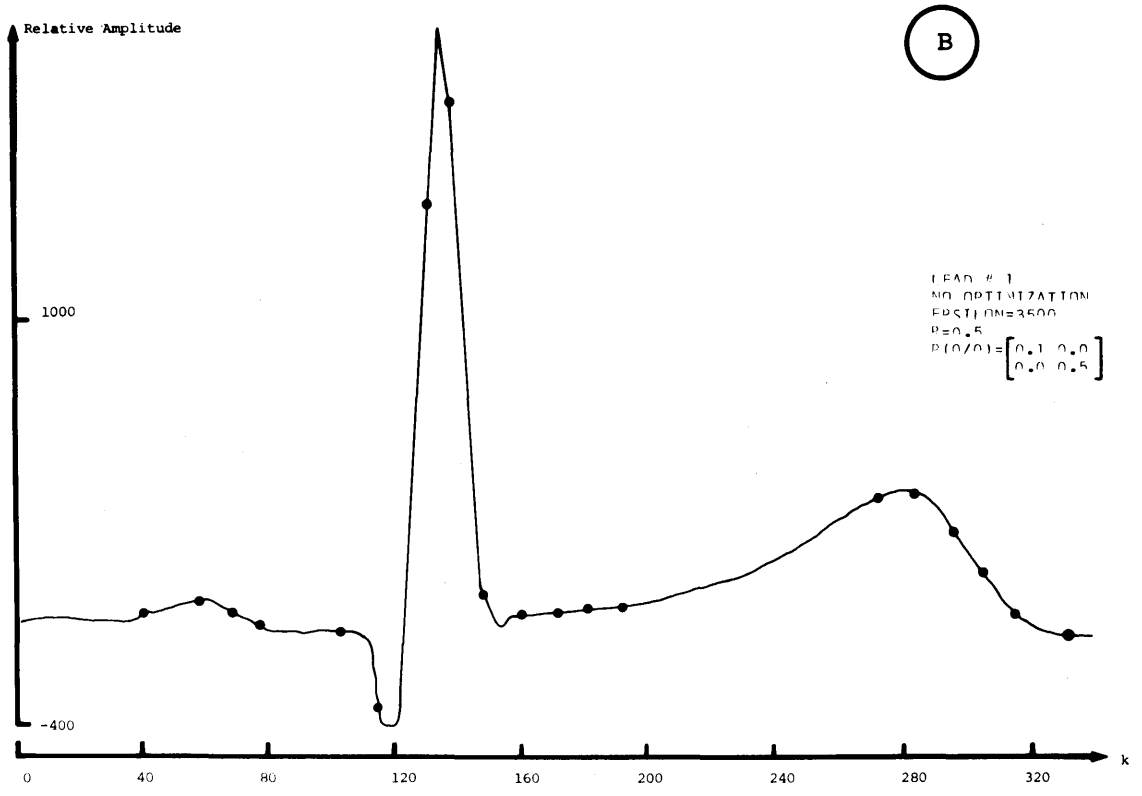
B
Relative Amplitude
1000
-400
LEAD # 1
NO OPTIMIZATION
EPSILON=3500
P=0.5
P(0/0)=[0.1 0.0
0.0 0.5]
0
40
80
120
160
200
240
280
320
k

Fig.VI.3

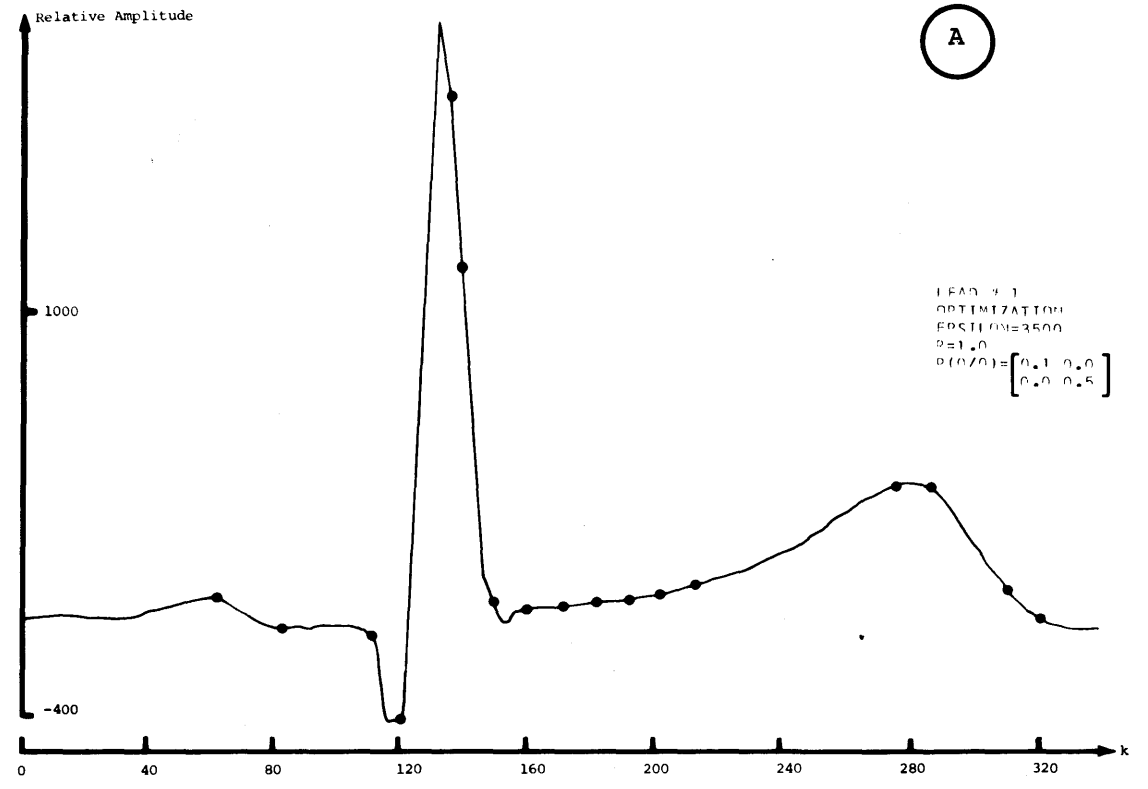
Relative Amplitude
A
1000
-400
LEAD # 1
OPTIMIZATION
EPSILON=3500
P=1.0
P(0/0)=
0.1 0.0
0.0 0.5
0
40
80
120
160
200
240
280
320
k

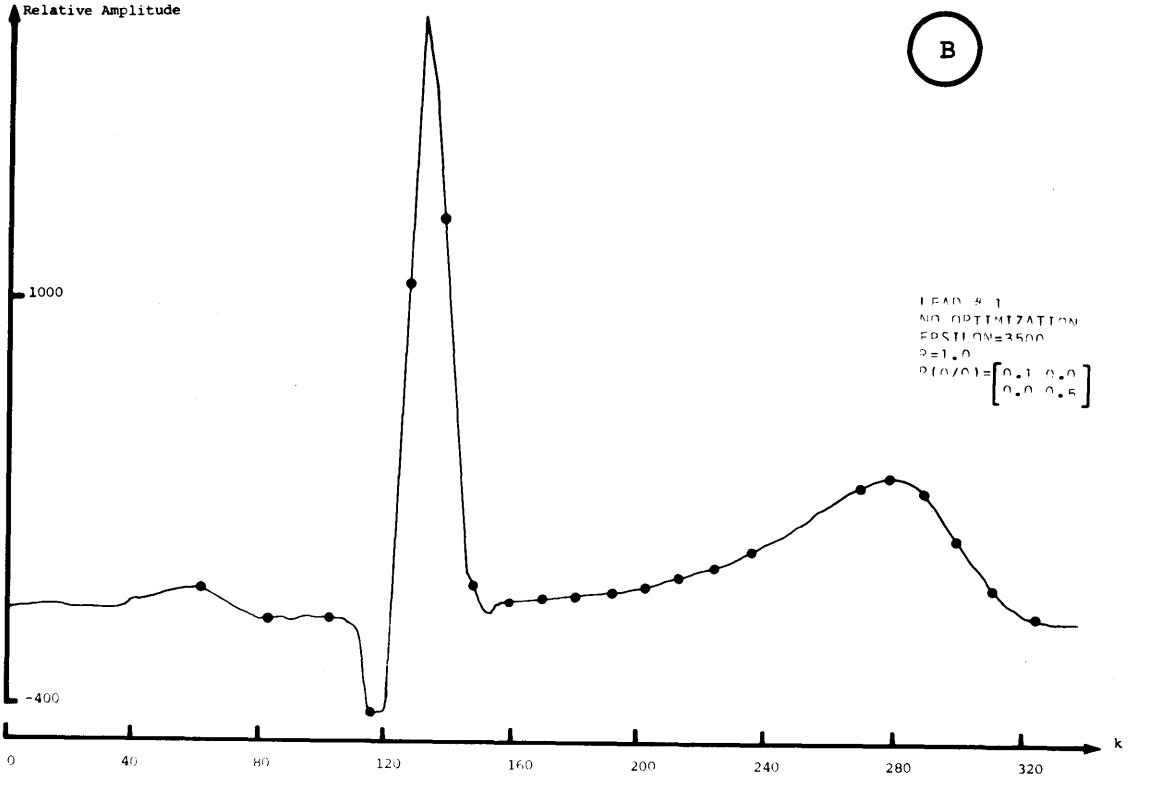
Relative Amplitude
B
1000
-400
LEAD # 1
NO OPTIMIZATION
EPSILON=3500
P=1.0
P(0/0)=
0.1 0.0
0.0 0.5
0
40
80
120
160
200
240
280
320
k

Fig.VI.4

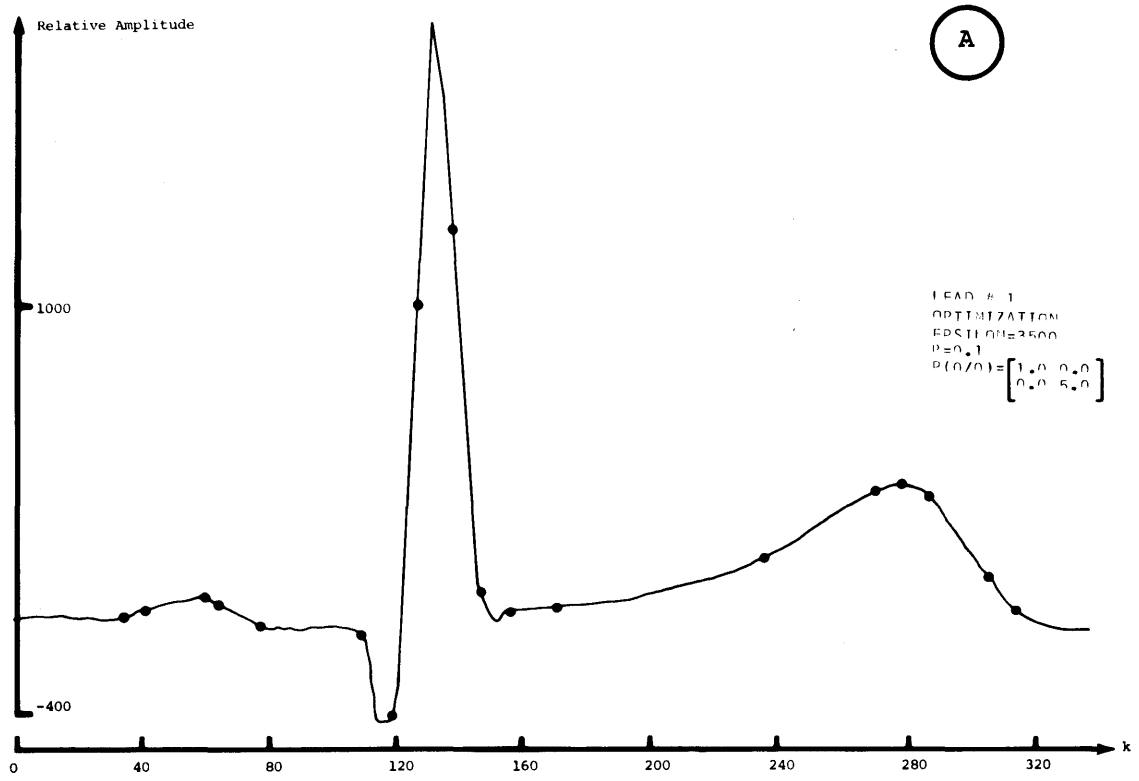
Relative Amplitude
A
1000
-400
LEAD # 1
OPTIMIZATION
EPSILON=3500
P=0.1
0
40
80
120
160
200
240
280
320
k

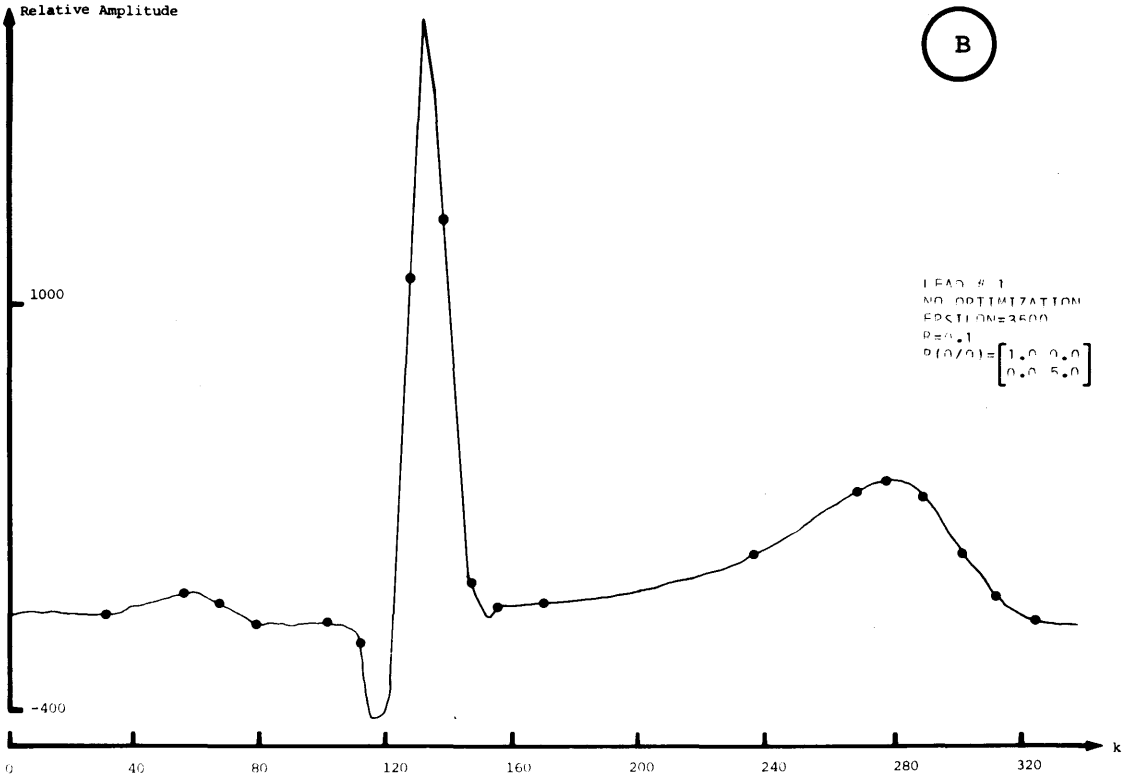
Relative Amplitude
B
1000
-400
LEAD # 1
NO OPTIMIZATION
EPSILON=3500
P=0.1
0
40
80
120
160
200
240
280
320
k

Fig.VI.5

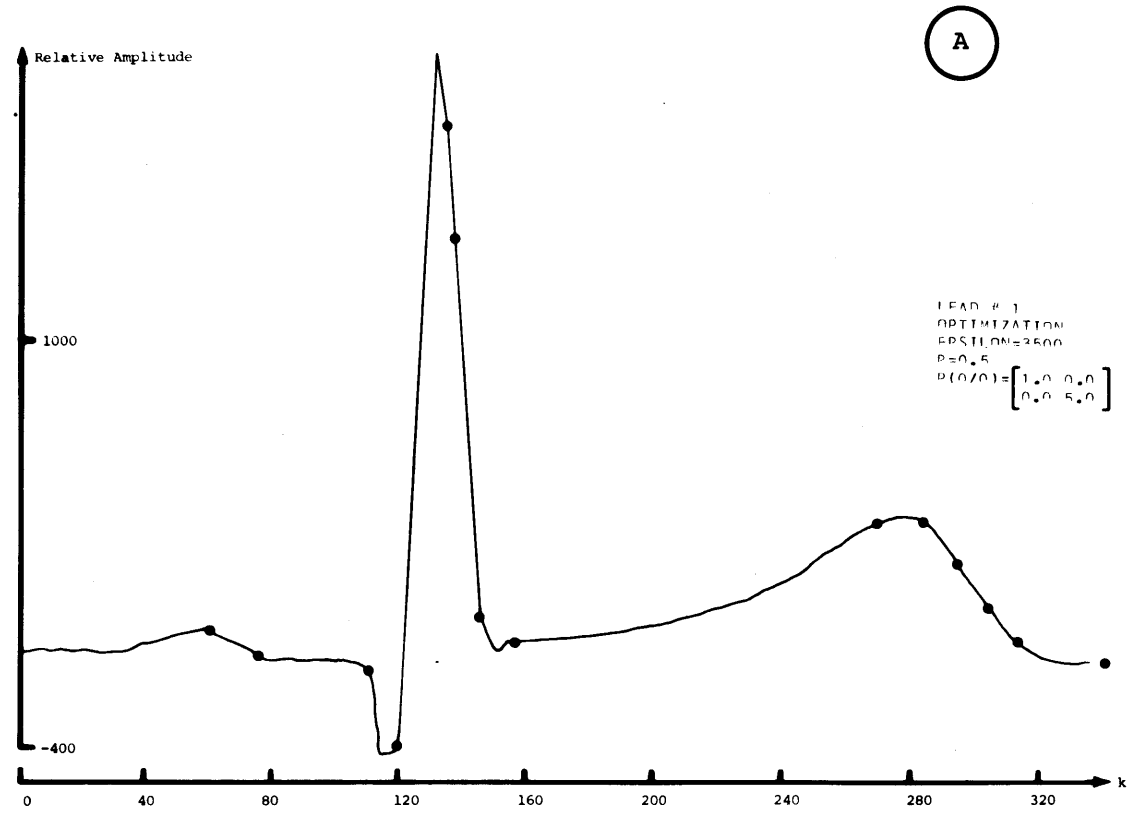
A
Relative Amplitude
1000
-400
LEAD # 1
OPTIMIZATION
EPSILON=3500
R=0.5
P(0/0)=[1.0 0.0
0.0 5.0]
0
40
80
120
160
200
240
280
320
k

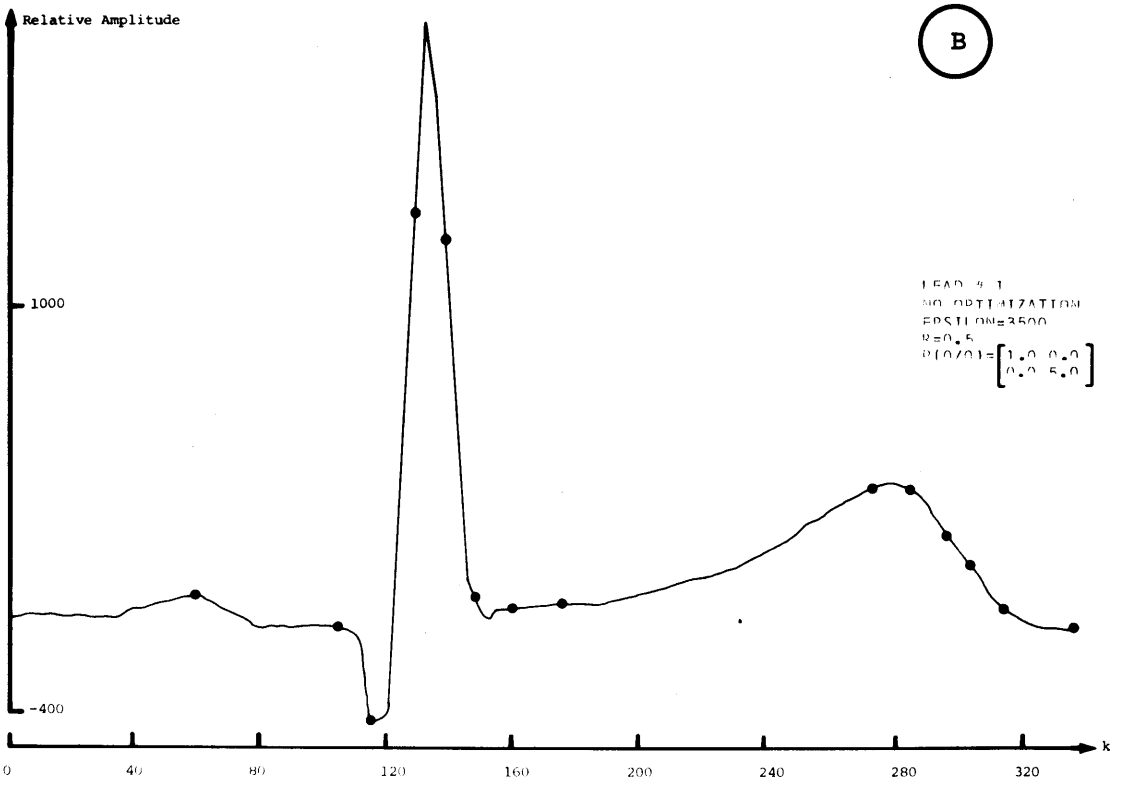
B
Relative Amplitude
1000
-400
LEAD # 1
NO OPTIMIZATION
EPSILON=3500
R=0.5
P(0/0)=[1.0 0.0
0.0 5.0]
0
40
80
120
160
200
240
280
320
k

Fig.VI.6

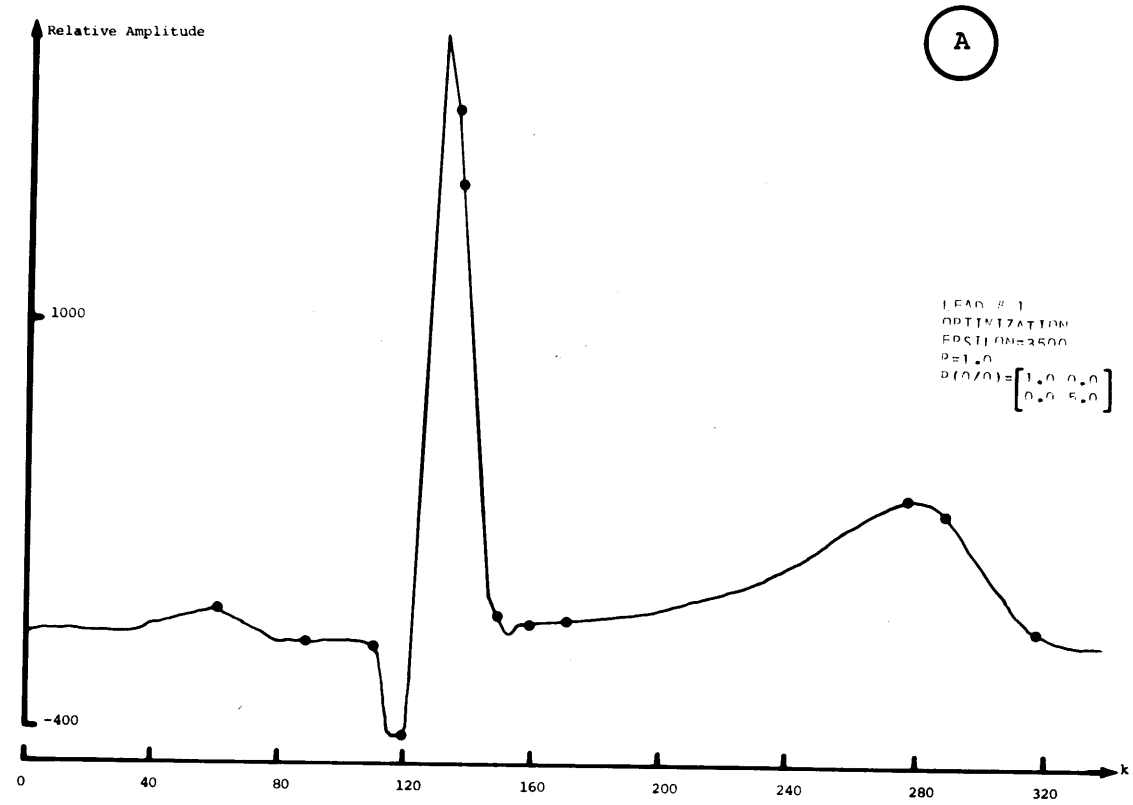
A
Relative Amplitude
1000
-400
LEAD # 1
OPTIMIZATION
EPSILON=3500
β=1.0
P(0/0)=
1.0 0.0
0.0 5.0
0
40
80
120
160
200
240
280
320
k

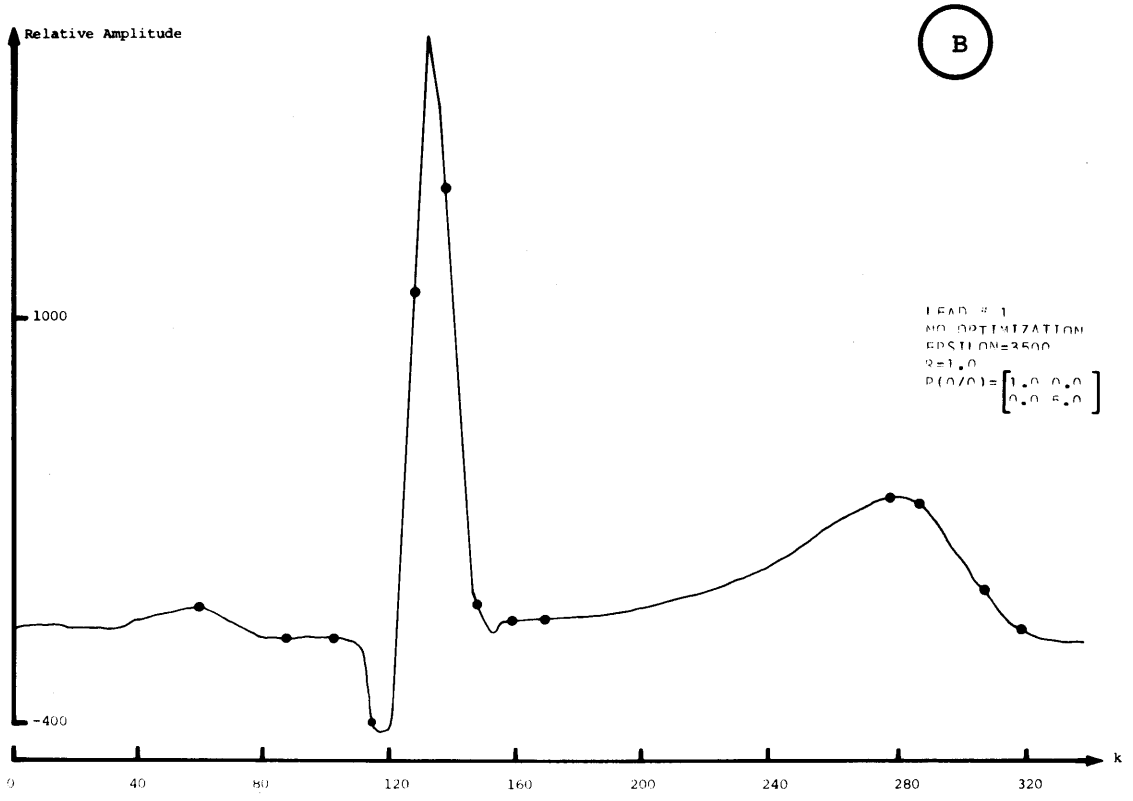
B
Relative Amplitude
1000
-400
LEAD # 1
NO OPTIMIZATION
EPSILON=3500
β=1.0
P(0/0)=
1.0 0.0
0.0 5.0
0
40
80
120
160
200
240
280
320
k

Fig.VI.7

D) As expected, given the high frequency content of the QRS Complex, -- the " knot density " in this region is high.

A detailed analysis of the tradeoffs involved in the choice of the de-- tection system parameters led us to consider :

a) small values of P(0/0) when using spline functions for ECG modeling (where we want more accurate estimation of the waveforms) , and

b) larger values of R, if one is mainly interested in defining the ti--- ming of cardiac events, i.e. specifically the sequence of waves (P,Q, R,S, and T), with less interest in the details of the shape of the -- waves. Note in this case we would prefer fewer knots so that we can -- more easily associate certain knots with specific cardiac events.

In order to fullfill the requirements of these two different approaches, the following sets of values were chosen :

SET A) Accurate ECG modeling :

$$R = 0.5 \quad , \quad P(0/0) = \begin{bmatrix} 0.1 & 0.0 \\ 0.0 & 0.5 \end{bmatrix}$$

Fig.VI.8 shows some real ECG data and its linear spline appro-- ximation using these set of numbers

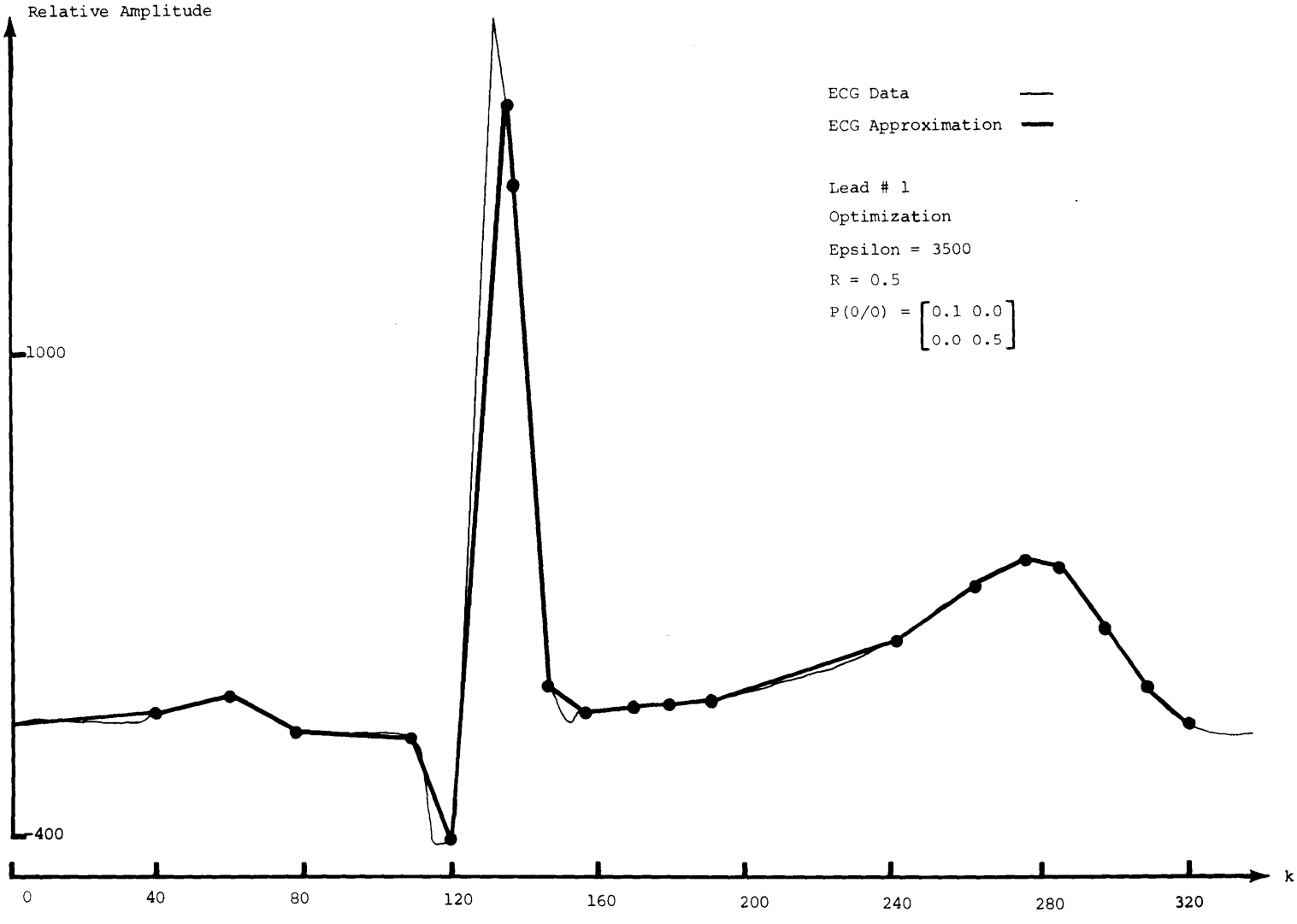
Relative Amplitude
ECG Data
ECG Approximation
Lead # 1
Optimization
Epsilon = 3500
R = 0.5
P(0/0) = [0.1 0.0; 0.0 0.5]
1000
400
0
40
80
120
160
200
240
280
320
k

Fig.VI.8

SET B) Timing of cardiac events (see Fig.VI.7a) :

$$R = 1 \quad , \quad P(0/0) = \begin{bmatrix} 1 & 0 \\ 0 & 5 \end{bmatrix}$$

VI.2) Time Varying Detection Law

Due to the fact that the range of values for the likelihood ratios $l(k,\theta)$ over a heartbeat cycle is too high (approximately 10^7), our unique -- decision rule VI.1.1 may provide misleading knot location information. To overcome this trouble we propose a time varying detection law of the form :

$$l(k,\theta) \underset{H_0}{\overset{H_1}{\gtrless}} \varepsilon(k) \qquad \text{(VI.2.1)}$$

over a single heartbeat cycle, with :

$\varepsilon(k) = \varepsilon_1$ for the QRS complex

$\varepsilon(k) = \varepsilon_2$ for the T wave

$\varepsilon(k) = \varepsilon_3$ for the P wave

We notice however, that the " on line " implementation of this time va-- rying decision rule requires some automatic procedure for defining the

sequence of waves (P,Q,R,S,and T) based on the sequence of knots , and the patient's heart-beat rate .

Some " off line " analysis tests using a variable treshhold $\varepsilon(k)$ were -- run in order to test the utility of this approach. Sets A) and B) were - chosen as the CGLR system parameters; optimization over a " data window" was performed. The following treshhold were chosen :

LEAD # 1 $\varepsilon_1 = 80000$

$\varepsilon_2 = 18000$

$\varepsilon_3 = 2500$

LEAD # 2 $\varepsilon_1 = 80000$

$\varepsilon_2 = 16000$

$\varepsilon_3 = 4000$

LEAD # 3 $\varepsilon_1 = 80000$

$\varepsilon_2 = 18000$

$\varepsilon_3 = 11000$

Data of two normal patients having the following characteristics were --- chosen :

PATIENT # 1 Heartbeat Rate = 50 Heartbeats/min

PATIENT # 2 Heartbeat Rate = 98 Heartbeats/min

Results for these patients are presented in Figs. VI.9 through VI.12 for both sets of system parameters A) and B). Some facts can be pointed out :

1) The CGLR detector locates more knots for the cectocardiogram (VCG) data of Patient #2 , since its heartbeat rate is greater than the ---- heartbeat rate of Patient #1 and we are actually looking at more ---- heartbeat cycles in the same time interval. (Compare Figs. VI.9 and - VI.11)
2) Use of normalized ECG data for all patients allows our detection sys-- tem to use fixed treshhold values in the time varying decision rules without affecting system performance, i.e. the sets of parameters A) and B) can be effectively used for ECG data processing for accurate -- ECG modeling and for defining the timing of certain cardiac events, -- respectively. Further work to verify this is needed.
3) Parallel knot location for the three Leads of the VCG may allow fur-- ther resolution of cardiac events. For example, since the P wave is -- not well defined in the data corresponding to Lead #3 , one can use -- the actual knot location of the first two Leads to identify it. More-- over, the QRS Complex can be identified by looking at the high " knot density " regions of the three Leads. (This information can be useful for implementing an automatic procedure for defining the sequence of - waves (P,Q,R,S,T). and the patient's heartbeat rate).


Patient # 1
R = 0.5
P(0/0) = [0.1 0.0]
[0.0 0.5]
Lead # 1
Lead # 2
Lead # 3
K
0
100
200
300
400
500
600
700
800
900
1000

Fig. VI.9


Patient # 1
R = 1
P(0/0) = [1 0; 0 5]
Lead # 1
Lead # 2
Lead # 3
K
0
100
200
300
400
500
600
700
800
900
1000

Fig.VI.10


Patient # 2
R = 0.5
P(0/0) = [0.1 0.0 / 0.0 0.5]
Lead # 1
Lead # 2
Lead # 3
K
0
100
200
300
400
500
600
700
800
900
1000
1100

Fig.VI.11


Patient # 2
R = 1
P(0/0) = [1 0; 0 5]
Lead #1
Lead # 2
Lead # 3
100
200
300
400
500
600
700
800
900
1000
1100
K

Fig.VI.12

Chapter VII

Conclusions

The failure detection analysis was performed in the context of a state space description of a spline used for ECG modeling. We have considered the spline function as a dynamic system driven by impulses, much as --- cardiac activity is driven by a series of impulses. This fact enabled - us to use the CGLR technique for locating knots.

Having recognized that the likelihood ratio $l(k,\theta)$ is a crucial quantity in the CGLR detection scheme, in Chapter II we initially analyzed some of its statistical properties, i.e. specifically the noncentrality pa-- -rameter $\delta^2(k,\theta,\theta_T)$.

In Chapter III we first considered the single knot location problem. There we developed a computer routine for computing the noncentrality parameter $\delta^2(k,\theta,\theta_T)$. As a result, we were able to get some practical insight into the nature of the CGLR detector and the tradeoffs involved to achieve " optimal " performance. We have also developed some ground- work for the multiple knot location problem, considering the special -- case in which we hypothesize two failures of equal size, i.e. $\alpha_1 = \alpha_2$. Examining the behavior of the noncentrality parameter $\delta^2(k,\theta,\theta_{T1},\theta_{T2})$ assuming different failures of different sizes remains for future work.

In Chapter IV we have also developed a framework in our search for the optimal values of the detection system's parametric vector $\alpha(0)$. In this

chapter, we have derived the sensitivity equations for the noncentrality parameter δ^2, but we again have only laid out some groundwork and much remains to be done (in particular we need a computer routine for com-- puting the sensitivity equations for the linear spline case; use of the computer package MAXIMA is suggested for obtaining the required quanti- ties in the sensitivity equations).

In Chapter V we studied the age weighting filtering concept. As a result , we were able to improve knot resolution getting some insight into the tradeoffs involved. It is our feeling, that the inclusion of age- ----- weighting greatly improves overall performance. The analytical work de- veloped in this research provided some understanding of CGLR performance in locating knots when we actually observe a spline in additive Gaussian noise. Thus, the first contribution of this thesis is an understanding of the theoretical properties of the CGLR system for knot location. We have studied the tradeoffs in system design, have isolated the critical design parameters, and have made several useful observations concerning system performance.

In Chapter VI we used this approach for approximating ECG's. A computer routine for the CGLR detector was written and used to process real ECG data. As a result, we were able to get additional insight into the trade- offs involved in :

a) using spline functions for ECG modeling, and

b) defining the timing of certain cardiac events.

Our results are quite encouraging, although we have only tested the system on a very small set of real data. Further experimentation is clearly needed. Nevertheless, we have been able to determine several sets of CGLR parameters that lead to good performance. One set of parameters leads to a substantial number (16) of knots per heartbeat but provides accurate ECG modeling with only linear splines. With the other set of parameters the CGLR system determines a smaller set of knots, which can then be used (together with the magnitudes of the likelihood ratios) to identify the sequence of waves in the ECG or VCG.

Further analysis tests for defining " optimal " values for the window --- size and the dead zone time interval for these two objectives is required An automatic procedure for defining the sequence of waves (P,Q,R,S, and T) , based on the sequence of knots, and the patient's heartbeat rate is also necessary.

Since VCG data actually provides simultaneous cardiac activity informa--- tion for three different leads, we could use a " spline vector " for VCG modeling. As this research did not consider this scheme, an analysis of CGLR similar to the one performed for the scalar case is desirable (and the present work provides the tools needed for such an approach).

Lastly, since the ECG model is a spline function $S_\theta(y,t)$ constrained to match exactly some set of ordinates y_i prescribed (see Chapter I) , our Kalman filter used to process ECG data will provide " best " estimates at

the locations θ_i of the detected knots. Thus, we may want to use " optimal smoothing " techniques [7] using all measurements between θ_{i-1} and θ_i to improve our estimate of the spline model at a certain time k, where $\theta_{i-1} < k < \theta_i$.

We feel that this research has clearly demonstrated the properties of -- CGLR for spline knot location and has provided a useful set of analytical tools. In addition, our application of CGLR to ECG data shows the promise of this method for heartbeat wave location and ECG data compression.

BIBLIOGRAPHY

1. Ahlberg.Nilson,Walsh, " The Theory Of Splines and their Applications " Academic Press, 1967

2. Schonberg," Cardinal Spline Interpolation " Conference Board of the Mathematical Science, SIAM, Philadelphia

3. Bueno,R.E.Chow,S.B.Gershwin and A.S.Willsky " Research Status Report to Nasa Langley Research Center : A Dual Mode GLR Approach to Self Reorganizing Digital Flight Control System Design " MIT, ESL, Camb. Mass. Nov. 1975

4. Detection and Identification of Transient Cardiac Arrythmias using Signal Analysis, Gustafson, Willsky and Wang , (CSDL) R-935

5. Cardiac Arrytmia Detection and Clasification through Signal Analysis, Gustafson, Willsky and Wang (CSDL) R-920

6. Willsky and H.Jones. " A Generalized Likelihood Ratio Approach to the Detection and Estimation of Jumps in Linear Systems " IEEE Transactions on Automatic Control, Feb. 1976

7. Jazwinski," Stochastic Processes and Filtering Theory " Academic Press 1970

8. Gustafson,Johnson and Akant " Cardiogram Analysis and Classification Using Signal Analysis Techniques " (CSDL) R-853 , Sept. 1974

9. Willems and Pipberger " Arrytmia Detection by Digital Computer " Comp. Biomed. Res. 5 : 263, 1972

10. A Primer of Electrocardiography, George E. Burch and Travis Winsor

5th Edition, Lea & Febiger, Philadelphia